climate

MDPI

Article

High-Resolution Temporal Variation of Thermal Discomfort Indices in the Eastern Mediterranean City of Athens, Greece, Since the Beginning of the 20th Century (1901–2024)

Basil E. Psiloglou *, Nikolas Gkinis and Christos Giannakopoulos

Institute for Environmental Research and Sustainable Development, National Observatory of Athens, P. Penteli, GR-15236 Athens, Greece; n.gkinis@noa.gr (N.G.); cgiannak@noa.gr (C.G.)

* Correspondence: bill@noa.gr

Abstract

This study analyzes more than a century of hourly meteorological data (1901–2024) from the Thissio station in central Athens, Greece, to assess the long-term changes in human thermal discomfort. Three simple and widely used bioclimatic indices, Thom's Discomfort Index (TDI), Humidex (HMDX), and Heat Index (HI), were calculated to capture the combined effects of air temperature and humidity. The results show a marked increase in the frequency, intensity, and duration of thermal discomfort since the 1980s, with a strong acceleration after 2000. The number of days with severe or dangerous heat stress has more than doubled compared with the mid-20th century, and periods of high discomfort now extend from June to September. The maximum values of HMDX and HI have exceeded critical health thresholds, highlighting increasing risks for the urban population. These findings demonstrate how rising temperature and humidity amplify heat stress in a Mediterranean city and emphasize the need for adaptation strategies in urban planning and public health to reduce vulnerability to extreme heat.

Keywords: climate change; thermal discomfort; discomfort indices; Thom's Discomfort Index; Humidex; Heat Index; Athens; Greece

check for updates

Academic Editor: Ying Li

Received: 7 August 2025
Revised: 20 September 2025
Accepted: 1 October 2025
Published: 6 October 2025

Citation: Psiloglou, B.E.; Gkinis, N.; Giannakopoulos, C. High-Resolution Temporal Variation of Thermal Discomfort Indices in the Eastern Mediterranean City of Athens, Greece, Since the Beginning of the 20th Century (1901–2024). *Climate* **2025**, *13*, 210. https://doi.org/10.3390/cli13100210

Copyright: © 2025 by the authors. Licensee MDPI, Basel, Switzerland. This article is an open access article distributed under the terms and conditions of the Creative Commons Attribution (CC BY) license (https://creativecommons.org/licenses/by/4.0/).

1. Introduction

The issue of climate change, which is driven by global warming, is of the utmost importance in the twenty-first century, having a profound impact on various aspects of human life, including public health [1]. The climate crisis is triggering changes in climate parameters, engendering shifts in thermal comfort that necessitate urgent climate action [2]. Climate change is a complex and dynamic process associated with many uncertain externalities [3,4]. It has been demonstrated that global warming and extreme weather events, such as storms and heat waves, are associated with climate change [5–9]. According to different scenarios, the world's temperature is expected to increase between 1.4 and 5.8 °C by the end of the twenty-first century, depending on the level of emissions [10,11]. It is particularly probable that heat waves and extreme precipitation are likely to occur with greater intensity [12]. Since the time of Herodotus (430 BC) it has been known that climatic conditions exert a combined effect on the human body, thereby increasing thermal discomfort and potentially impacting health [13–16]. This makes it especially important to investigate changes in thermal comfort, particularly in outdoor applications.

Human comfort depends upon physiological, psychological, and behavioral conditions [17]; hence, it is challenging to define the term human comfort. The most extensively

recognized definition of human comfort is "The condition of mind, which expresses satisfaction with the thermal environment" [18]. The human body experiences comfort when the environment is maintained in a manner that facilitates the body's ability to swiftly attain thermal balance with its surroundings. When the body's heat gain exceeds its thermoregulatory capacity, body temperature begins to rise, potentially leading to heat-related illnesses and disorders. The body may attempt to cool down by varying the rate and depth of blood circulation, by losing water through the skin and sweat glands, or as a last resort, by panting. Sweating plays a crucial role by cooling the body through the process of evaporation. However, high relative humidity can impede evaporation by diminishing the body's ability to cool itself effectively. The body's thermoregulatory ability varies considerably with gender, age, and size. Activity level and clothing also have a significant impact on thermal comfort.

Achieving thermal comfort from a climatological perspective hinges on factors like temperature, humidity, wind speed, solar radiation, metabolic heat, and clothing conditions [19] with temperature and humidity being the most influential for human comfort and health [20]. For this reason, several thermal comfort indices have been developed which translate meteorological data into scales that reflect people's responses to weather conditions, ranging from very comfortable to very uncomfortable [21–27]. These indices simplify the interpretation of atmospheric effects on human comfort and facilitate comparisons between different regions [28]. Alerts are typically issued when a heat stress index is forecasted to exceed a specific threshold. Examples of heat stress indices which are suitable for warm environmental conditions are Thom's Discomfort Index (TDI) [29], Canada's Atmospheric Environment Service Humidex (HMDX) [30], and NOAA's (U.S.A. National Oceanic and Atmospheric Administration) Heat Index (HI) [31–33].

TDI, the first physiological index of this kind presented in 1959, is based on the conditions of air temperature and relative humidity [34,35] and expresses their combined contribution to human thermal comfort [36] and is easier to be evaluated, especially at a comparative level. For these reasons, TDI has been adopted in various parts of the world, with different climatological conditions. Yousif and Tahir [34], using TDI, investigated the thermal effect on people in Khartoum, Sudan. Adegoke and Dombo [37] examined human thermal comfort in Akure, Nigeria. Talukdar et al. [38] applied TDI to assess the trend of outdoor thermal discomfort in Mymensingh City, Bangladesh, during 2006–2015. Ehsan et al. [39] applied TDI to evaluate thermal discomfort levels, building design concepts and some heat mitigation strategies in low-income neighborhoods of Faisalabad, Pakistan. Monforte et al. [40] used TDI to characterize from the prospective bioclimate the provinces that make up the island of Sicily in South Italy, a Mediterranean region defined as a hotspot of climate change. Maftei et al. [41] used TDI to establish the thermal comfort or thermal discomfort conditions for the coastal zone of the Black Sea, in the Dobrogea region (Romania). Azevedo et al. [42] used TDI to evaluate the thermal conditions of urban areas in Petrolina-PE, Brazil, for the year of 2012.

HMDX, developed at Canada's Atmospheric Environment Service (now the Meteorological Service of Canada) in 1979, is a relatively simple index that relies only on temperature and relative humidity, making it easier to calculate than more complex indices like the Universal Thermal Climate Index (UTCI) and the Wet-Bulb Globe Temperature (WBGT). By combining air temperature and humidity, the Humidex offers a more accurate representation of how weather conditions feel to individuals, particularly in humid environments. Due to its simplicity, HMDX has also been used in climatologically different areas worldwide. Diaconescu et al. [43] proposes an approach that enables the reliable estimation of the daily HMDX index, using daily temperature and humidity data in Canada. Orimoloye et al. [44] appraised the indications of climate variability and heat stress index on human health incorporating HMDX for the period of 1986 to 2016, over East London, South

Africa. Golbabaei et al. [45] and Fallah Ghalhari et al. [46] used HMDX to demonstrate a comprehensive view of the heat stress in Iran, analyzing meteorological data for two periods, 1965–2009 and 1985–2014, respectively. Scoccimarroet al. [47] applied HMDX to include the effect of humidity on the temperature perceived by the human body under moderate to extreme conditions, in exposed areas over Europe. Středová et al. [48] used HMDX to evaluate the impact of an urban heat island on the residents and visitors of Hradec Králové, Czech Republic. Infusino et al. [49] used HMDX to analyze the combined effects of temperature and relative humidity on people living in the Crati River valley (south Italy), a very interesting area for its territorial, climatic, and socioeconomic particularities.

HI, also known as the apparent temperature, described by Lans P. Rothfusz [33] in a 1990 U.S.A. National Weather Service Technical Attachment after analyzing original data tables of apparent temperature proposed in 1979 by Steadman [31], is what the temperature feels like to the human body when relative humidity is combined with the air temperature. This has important considerations for the human body's comfort, and because of this, it has been used as a measure of heat exposure in studies throughout the world. Dahl et al. [50] applied HI to evaluate the increase in frequency and exposure of the population to days with extreme heat in the United States during the 21st century. Michelozzi et al. [51] used HI to evaluate the impact of high environmental temperatures on hospital admissions during April to September in 12 European cities. Khalaj et al. [52] used this index to determine and characterize the health impacts of extreme heat events on the population in five regions of New South Wales, Australia. Kyselý et al. [53] also applied HI to examine heat-related mortality in the population of South Korea between 1991 and 2005 and examine the extent to which the 1994 heat wave was unusual in terms of mortality impacts and recurrence probability. Bell et al. [54] also used this index to investigate heat-related mortality for three Latin American cities (Mexico City, Mexico; São Paulo, Brazil; Santiago, Chile).

Several studies have also examined thermal discomfort in Greece, which possesses a Mediterranean climate, characterized by cool and wet winters and hot and dry summers. Angouridakis and Makrogiannis [55] determined the environmental thermal sensation for summer in Thessaloniki by analyzing air temperature and relative humidity data for the period 1950–1957. Tsitoura et al. [56] performed outdoor questionnaires about the thermal comfort effect on people in four cities of Crete. Matzarakis and Mayer [57] examined heat stress in Greece, for 12 selected synoptic stations of the Greek Weather Service, using the Predicted Mean Vote (PMV) thermal index. Kambezidis et al. [58] investigated the future thermal sensation of the Greek population, using TDI, for 33 locations in Greece (including Athens), incorporating input data from Typical Meteorological Years (TMYs) developed specifically for each location for meteorology–climatology applications [59]. Each TMY consists of a set of typical meteorological months (TMMs) selected from individual years covering a period of 30 years (1985–2014), integrated into a complete year, reflecting all the climatic information of the location for a period as long as the mean life of the system.

Specifically, for Athens there have been several studies about the effect of heat-related stress on the population. Giles et al. [60] examined the heat waves that affected Athens (and Thessaloniki) in July 1987 and July 1988 using TDI and the "relative strain" index. Paliatsos and Nastos [61] compared the thermal effect during air pollution episodes in Athens during the summers of 1993–1995 using TDI and found that it was related to the ozone concentration. Tselepidaki et al. [62] examined the summer thermal perception in Athens for cooling purposes using TDI. Bartzokas et al. [63] examined the characteristics of the inter-annual and intra-annual variability of thermal discomfort in Athens for a longer time period, utilizing the PMV discomfort index. Stathopoulou et al. [36] explored the use of thermal AVHRR satellite data to map bioclimatic comfort conditions by estimating TDI, for the case of Athens. Matzarakis and Nastos [64] analyzed heat waves in Athens

during 1955–2001 using the daily physiologically equivalent temperature (PET) index and the daily minimum air temperature, presenting an increasing trend in heat wave frequency, with heat waves being more pronounced since the mid-1970s. Nastos and Matzarakis [65] investigated whether there is any association between daily mortality and air temperature and thermal indices such as PET and Universal Thermal Climate Index (UTCI) within the wider region of Athens, Greece, for a 10-year period, 1992–2001. Pantavou et al. [66] used various thermal comfort indices in Athens (see Table 2 in [66]). Also, Pantavou et al. [67] estimated the thermal sensation of pedestrians in four locations of Athens using UTCI. From a time scale perspective, previous studies have mainly focused on a daily basis or certain hours of the day. Katavoutas and Founda [68] using hourly values of air temperature, relative humidity, and solar radiation for Athens, examined a smaller period of 1960–2017, and found an increasing risk of heat stress in Athens using two simple (HMDX, HI) and two rational (UTCI, PET) indices.

Based on the existing background knowledge, this research aims to explore the temporal variation in thermal sensation and discomfort in Athens, Greece. By using one of the oldest, largest, and most homogeneous meteorological datasets for an urban environment in the Mediterranean, the present study attempts to make a significant contribution to the research on thermal discomfort. The combination of the large temporal coverage, more than a century (1901–2024), and the high resolution of this dataset, 1 h time step, enables a reliable analysis of both long-term climate trends and short-term thermal extremes, offering an evidence-based perspective that complements and extends already-existing studies based on daily data or shorter time intervals. Three simple and widely known discomfort indices, TDI—the first physiological index of this kind introduced— and HMDX and HI—both used operationally on our days for excessive discomfort warnings—have been analyzed across the globe in areas with different climatology, thus adding an important dimension to traditional temperature-based climate studies, offering a differentiated perspective on how climatic factors interact and affect human comfort and environmental stress in the region. The revealed changes in thermal discomfort levels in the region provide valuable insights into potential impacts on public health. These elements reinforce the scientific value of the present research, positioning Athens as a representative case study for Mediterranean metropolitan areas experiencing intensified heat stress due to urbanization and climatic change.

2. Materials and Methods

2.1. Data Sources

The present analysis was based on meteorological data records from Thissio meteorological station, maintained by the National Observatory of Athens (NOA), Greece (latitude: 37°58′ North, longitude: 23°43′ East), for more than a century. The station is located on a small hill near the Acropolis at an elevation of 107 m above mean sea level. The distance to the coastline is about 5 km. Although the station lies near the center of Athens, it is isolated from heavy traffic and densely built areas.

Specific information on the observation methods and measuring instruments employed for the measurement of air temperature and humidity parameters at Thissio meteorological station, since its commencement of operation, is provided in Appendix A [69–73]. In May 2017, according to a list of criteria, Thissio station was recognized by the World Meteorological Organization (WMO) as a long-term observing station for its high-quality climate records (WMO Decision 8, EC-69, May 2017).

Although air temperature is usually used to express a component of thermal comfort, it is rarely the reason for heat stress by itself alone [74]. Sweating plays a key role in the body's thermoregulatory process by cooling the body through the process of evaporation.

However, high relative humidity retards evaporation, reducing the body's ability to cool itself. Thus, both temperature and relative humidity parameters are necessary for the calculation of thermal discomfort indices, due to their dominant role in determining human heat perception.

For the needs of this study, measurements of air temperature and relative humidity at a 1 h time step were collected and analyzed, covering a period of 124 years, 1901–2024 (in Local Standard Time, LST = GMT + 2 h). Although the long-term air temperature time series has been checked for its homogeneity and accuracy [73], an extra extensive quality control was performed on temperature–humidity pairs, checking and correcting any erroneous values that may have passed automated procedures. Based on input parameter availability (1 h temperature and humidity pairs), a total of 1,079,938 calculated indices were analyzed, with missing values corresponding to less than 0.65%.

Athens, the capital and the largest city in Greece, is located in a region of complex topography within the Athens basin (~450 km^2), presenting an elongated shape spanning from the NE to the SW direction, surrounded by mountains ranging in height from 400 to 1500 m at the western (Aegaleo, 458 m), northern (Penteli, 1107 m), and eastern (Imitos, 1026 m) sides. The city is also open to the sea to the south (Saronikos Gulf) and is close to the port of Pireaus (Figure 1). To the east of the basin's axis, the city is less densely populated. To the west, the area is designated as 75% industrial and 25% residential. Athens enjoys a typical Mediterranean climate with mild winters (DJF) (December, January, February; mean seasonal air temperature of 10.1 °C) and warm summers (JJA) (June, July, August; mean seasonal air temperature of 26.1 °C). The annual rainfall is approximately 376 mm, with the majority occurring in early October and the winter months. However, during the summer months, occasional severe local thunderstorms of short duration may also contribute to significant precipitation [75]. The Athens region experiences an average of 2919 h of sunshine per year. The prevailing winds in the Athens basin blow from N and NE in late summer, fall, and winter and from SSW and SW in the spring and early summer. It is important to note that these NE and SW directions coincide with the major geographical axis of the basin. The basin's ventilation is inadequate during periods of local circulation systems, such as sea–land breezes along the major NE–SW geographical axis of the basin. Kallos et al. [76] and Kassomenos et al. [77] cited additional information on the flow regime and the structure of the boundary layer over Athens.

In 2001, the population of Athens' urban area was 3.7 million, accounting for more than one-third of the country's total population. The surface area of the site was measured at 433 Km^2, and it continues to expand at an accelerating rate. According to Eurostat, the Athens metropolitan area is the eighth most populous in the European Union, with a population of approximately 4 million inhabitants in 2004. However, this number is expected to increase due to the presence of a significant number of undocumented migrants in the city. Despite some attempts toward decentralization between 1980 and 1990, Athens remains the center of the country's commercial, economic, industrial, political, and cultural activities. Figure 2 presents the population growth of Athens since the mid-19th century (data are provided in Appendix A) [78–82]. The city's rapid growth, particularly after World War II, was accompanied by a large number of automobiles, leading to poor air quality and traffic problems.

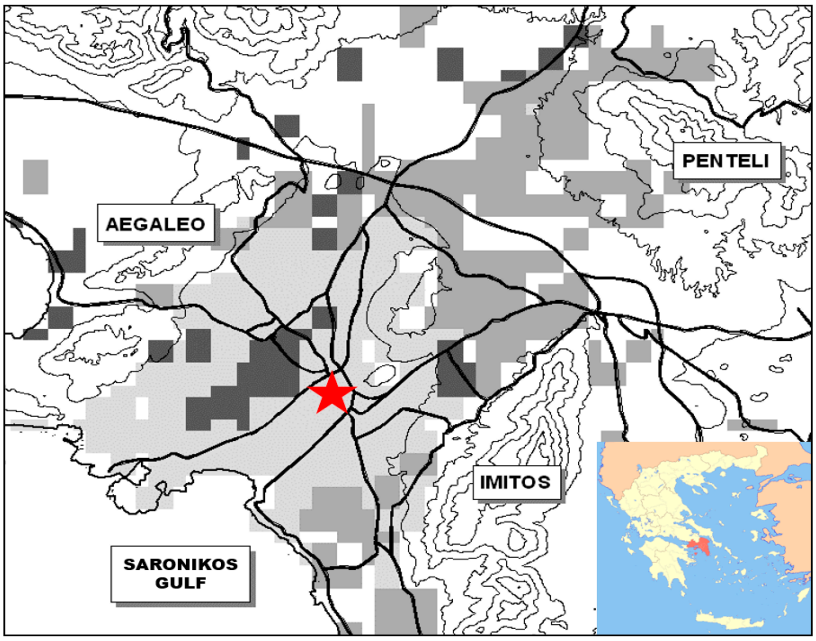

Figure 1. Map of the greater Athens area, where the location of the historical station of the National Observatory of Athens (NOA) in the Thissio area is marked (red star). Urban areas are marked with light gray, semi-urban areas with medium gray, and finally, industrial areas are marked with dark gray.

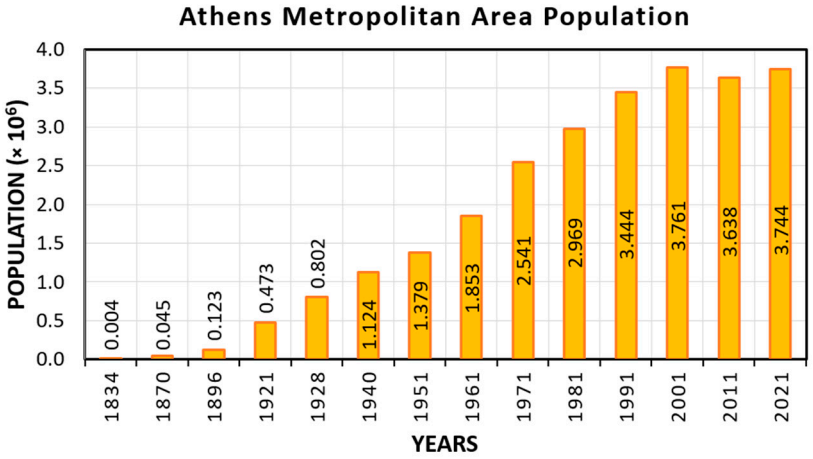

Figure 2. Population of the Greater Athens metropolitan area since the middle of the 19th century (sources: [78–82]).

Over the past few decades, Athens has experienced regional climate change along with significant urbanization. However, a delayed summer temperature increase in the eastern Mediterranean relative to the western Mediterranean has been observed, attributed to the increased frequency of northerly winds from the mid-1960s to mid-1980s [83]. This feature is a notable aspect of the observed climate change in this region. The observed increase in Athens' mean temperature began in the mid-1980s [84]. Moreover, the ongoing process of urbanization and its associated urban heat island effect serve as a secondary contributor to the local warming and the modification of climate characteristics, particularly during the summer months. A potential factor that could affect the climate in Athens is the recent destruction of a significant portion of the green areas located on the northern outskirts of the city, which was caused by the recent forest fires.

2.2. Thom's Discomfort Index (TDI)

The subjective sensations of comfort and discomfort are influenced by individual perceptions and external weather conditions. The American Society of Heating, Refrigeration and Air Conditioning Engineers (ASHRAE) has developed the concept of "effective temperature" over the course of several years. This concept is thoroughly discussed in ASHRAE [85], where it is defined as follows: "An empirically determined index of the degree of warmth perceived when exposed to different combinations of temperature, humidity and air movement". Research by Bosen and Thorn of the U.S. Weather Bureau, as described by Thom in 1957 [86], demonstrated that a simple linear equation based on dry- and wet-bulb readings yielded values that closely approximated the effective temperature over a range of temperatures and relative humidities commonly experienced in the U.S. during summer. The original equation

$$\mathrm{TDI} = [(\mathrm{Ta} + \mathrm{Tw})/2] + 0.1 \times [-150 - (\mathrm{Ta} + \mathrm{Tw})] \quad (1)$$

is usually simplified to

$$\mathrm{TDI} = 0.4 \times (\mathrm{Ta} + \mathrm{Tw}) + 15 \quad (2)$$

where Ta is the dry-bulb temperature in °F and Tw the wet-bulb temperature in °F.

Alternative versions have been proposed for use with air temperatures measured in °C and/or humidities described in terms of relative humidity expressed in %. The following mathematical expression was used:

$$\mathrm{TDI} = \mathrm{Ta} - 0.55 \times (1 - \mathrm{RH}/100) \times (\mathrm{Ta} - 14.5) \quad (3)$$

where Ta is the air temperature in °C and RH is relative humidity in %.

In a subsequent article, Thom [29] provided a list of boundary values that indicated degrees of discomfort. These are presented in Table 1, where the discomfort index is based on the Celsius temperature scales. Since these values were formulated for the U.S., they may also be considered valid for countries at a similar latitude, such as Greece.

Table 1. Thom's Discomfort Index classes, ranges, and description.

Range (°C)	Discomfort Level
TDI < 21	No discomfort
21 ≤ TDI < 24	Under 50% of the population feels discomfort
24 ≤ TDI < 27	Over 50% of the population feels discomfort
27 ≤ TDI < 29	Most of the population suffers discomfort
29 ≤ TDI < 32	Everyone feels severe stress
TDI ≥ 32	State of medical emergency

2.3. Humidex Index (HMDX)

Humidex, created by Canadian meteorologists, was initially used to describe how humidity affects human comfort. On a warm day, high relative humidity can make it feel even hotter because perspiration does not evaporate easily. When the Humidex value exceeds 38 °C, it is considered an extreme weather event. The threshold of HMDX ≥ 38 °C was used by Giannakopoulos et al. in 2011 [87] to identify days with significant thermal discomfort, as it marks a level where human health may be adversely affected, especially during prolonged outdoor exposure. This threshold aligns with guidelines from Environment Canada [88], which is used operationally for its excessive discomfort warnings, and is widely adopted in climate–health impact assessments and extreme heat studies. At a Humidex value of 30 °C, outdoor activities should be carefully managed, paying particular

attention to the elderly and children and the overall health of adults [88]. The Humidex value represents an equivalent temperature, indicating how hot it feels to the human body by factoring in both temperature and relative humidity. The equation for calculating the Humidex was proposed by Masterson and Richardson [30]. The HMDX index is calculated using the following Equation (4), which is valid for air temperatures above 21 °C, and the interpretation of its range is detailed in Table 2.

$$\text{HMDX} = \text{Ta} + (5/9) \times (\text{e} - 10) \quad (4)$$

where Ta is the air temperature in °C and RH is relative humidity in %, and e is the vapor pressure given by the expression

$$\text{e} = 6.112 \times 10^{(7.5 \times \text{Ta}/(237.7 + \text{Ta}))} \times \text{RH}/100 \quad (5)$$

Table 2. HUMIDEX classes, ranges, and description.

Range (°C)	Discomfort Level
HMDX < 20	No discomfort
20 ≤ HMDX < 30	Little to no discomfort
30 ≤ HMDX < 38	Some discomfort
38 ≤ HMDX < 45	Great discomfort, avoid exertion
HMDX ≥ 45	Dangerous, heat stroke quite possible

2.4. Heat Index (HI)

The Heat Index (also known as Steadman's Apparent Temperature) is one of the most popular indices used in environmental health research [31,32,89], a variant of which serves as the foundation for heat advisories in numerous communities across the United States [90]. HI translates current weather conditions (air temperature and air moisture in the most basic formulations) into the air temperature that would "feel" the same to humans if the dew point temperature was 14 °C [31,33]. Steadman's approach involved expressing weather conditions in terms of the equivalent temperature if the dew point temperature was 14 °C. This method enabled Steadman to translate combinations of air moisture and temperature, as well as other factors such as wind speed and sun radiation, into a single scale [31,32], measured in the same units as air temperature. This index is a simplified version that relies exclusively on air temperature and moisture [31].

The formula for the HI was developed based on work conducted in the late 1970s. The R. G. Steadman paper entitled "The assessment of sultriness" employed a list of twenty factors to determine a person's perceived temperature on a given day. These factors included the rate of sweat production, the type of clothes worn, the surface area of the body, and the activity being performed. Meteorologists within the U.S. National Weather Service used Steadman's table to derive a simpler formula for HI. They did so by creating a mathematical formula that approximates its values, within ±0.7 °C (±1.3 °F), using only two variables—air temperature and percent relative humidity—being valid for air temperatures above 20 °C:

$$\begin{aligned}\text{HI} = c_0 + (c_1 \times \text{Ta}) + (c_2 \times \text{RH}) + (c_3 \times \text{Ta} \times \text{RH}) + (c_4 \times \text{Ta}^2) + (c_5 \times \text{RH}^2) + \\ (c_6 \times \text{Ta}^2 \times \text{RH}) + (c_7 \times \text{Ta} \times \text{RH}^2) + (c_8 \times \text{Ta}^2 \times \text{RH}^2)\end{aligned} \quad (6)$$

where Ta is the air temperature in °C and RH is relative humidity in %, and constants c_i take the values of

$c_0 = -8.784695$, $c_1 = 1.61139411$, $c_2 = 2.338549$, $c_3 = -0.14611605$, $c_4 = -0.012308094$, $c_5 = -0.016424828$, $c_6 = 0.002211732$, $c_7 = 0.00072546$ and $c_8 = -0.000003582$.

The development of the HI was not intended to study human health, but rather to measure thermal comfort [91]. However, it has gained traction as a prevalent exposure metric in the field of environmental health. The U.S. National Weather Service (NWS) has established a correlation between distinct Heat Index values and environmental health hazards. For instance, a Heat Index of 41 °C indicates a "danger" level associated with heat-related medical complications [92]. The NWS utilizes HI for its operational excessive heat warnings [93]. The interpretation of its range, with the assumption that the individual is healthy and has easy access to water and shade, is outlined in Table 3. Accidental exposure to full sunshine could increase HI values by up to 8 °C [94].

Table 3. Heat Index classes and description, with shaded caution/danger ranges.

Range (°C)	Discomfort Level
HI < 27	No effect—temperature and humidity should not have any effect.
27 ≤ HI < 32	Caution: fatigue is possible with prolonged exposure and activity. Continuing activity could result in heat cramps.
32 ≤ HI <41	Extreme caution: heat cramps and heat exhaustion are possible. Continuing activity could result in heat stroke.
41 ≤ HI < 54	Danger: heat cramps and heat exhaustion are likely; heat stroke is probable with continued activity.
HI ≥ 54	Extreme danger: heat stroke is imminent.

2.5. Methodology

This study applies a detailed and reproducible methodology to examine thermal discomfort over Athens, Greece, over a historical period spanning more than a century (1901–2024), incorporating high-resolution meteorological records. The three widely recognized bio-meteorological indices (TDI, HMDX, HI) were calculated for the entire study period, whenever the Ta-RH pair was available, in 1 h intervals, using FORTRAN code especially developed for this purpose. All index results were kept with one decimal place, maintaining the same decimal precision as the air temperature values in the historical archive. The relative humidity values were provided as integers.

The main differences between the three indices (TDI, HMDX, and HI) lie in their composition, limits, and functional use. The TDI is the oldest and simplest index proposed in 1959 by Thom [29], primarily designed to describe discomfort at the population level (e.g., what percentage of people feel stressed) and historically used in many regions due to its ease of calculation and interpretation. On the other hand, HMDX, developed with clearly defined health-related thresholds [30], tends to be more sensitive to high humidity than TDI, thus offering the enhanced capture of discomfort in humid heat conditions. Finally, the HI, employing a more sophisticated expression in order to approximate human thermal equilibrium, also based on air temperature and relative humidity [31,33], produces thresholds that are directly linked to health advisories. Its extensive utilization in global environmental health research has led to its adoption as a policy-oriented and health-focused tool.

With regard to the question of representativeness, it is not possible to consider any index to be universally superior, as each index has its own advantages, depending on the application. In our framework (Athens metropolitan city with a Mediterranean climate) the TDI is useful for historical comparability and evaluating relevant trends over long periods of time. HMDX and HI, incorporating an enhanced weighting of humidity and utilized directly in operational health warnings, may prove more representative of actual perceived heat stress and health risks. The HI is more widely used in epidemiological and public health studies, while HMDX is simpler to calculate and more common in climatological studies outside the U.S. Therefore, in this study, our approach of analyzing all three indices

in parallel provides a more comprehensive and comparative perspective: TDI ensures long-term comparability, HMDX highlights humidity-driven thermal stress, and HI directly links to health advisories and epidemiological evidence.

Having available Ta and RH as input parameters and three index (TDI, HMDX, HI) values in 1 h intervals, the average, maximum, and minimum values per day and parameters were calculated, but only if hourly values per day exceeded 80% availability (i.e., at least 19 out of 24 values were available). In instances where the availability was less than 100%, we also verified whether the missing air temperature values were during midday, as this would affect the daily maximum value and our subsequent analysis.

To characterize both short-term variability and long-term climate trends, the indices were analyzed on a daily, monthly, seasonal, annual, decadal, and twenty-year basis. The daily scale identifies daily fluctuations, extreme events, and threshold exceedances related to human health. The monthly scale highlights intra-annual variability, identifying the months with the highest risk of thermal discomfort. The seasonal scale focuses on climatologically critical periods (e.g., July and August), assessing changes in the intensity of seasonal heat stress. The annual and decadal scales smooth out variability over time, providing a reliable long-term picture of climate change. For the most recent decade, the results for the four-year period 2021–2024 have been included into the decade 2011–2020. The multi-climate approach allows for a comprehensive examination of how urbanization and climate change have influenced discomfort trends over more than a century.

To quantify extreme heat or discomfort events, the 90th or the 95th percentile of temperature (or daily maximum temperature) is widely adopted in climatological and bio-meteorological studies, guidelines, or practical applications as a threshold, representing conditions that are statistically extreme but frequent enough to be important for adaptation and planning. This approach standardizes thresholds for extreme heat events, aligns with health impacts, and accounts for regional variability [95,96]. The 90th percentile of temperature is generally better for ensuring consistency across heat stress indices like Heat Index and Humidex in most operational contexts, as it captures a broader range of extreme events, aligns with public health warnings, and is widely supported by studies [96–102]. The 95th percentile is preferable for rare, high-severity events, particularly in hot climates or for climate change projections [103,104].

By clarifying the analytical structure and decision-making process, this expanded methodology enhances the relationship between the detailed results presented in the following sections and a transparent, reproducible framework.

3. Results and Analysis

3.1. Distribution of Thermal Discomfort Indices per Day—Thermal Stress Calendars

In order to emphasize the identification of seasonal variations and periods with the highest risks of thermal discomfort per index, a classification of each day in the examined period is performed, based on its daily maximum discomfort value. This classification follows the categories presented in Tables 1–3 for each discomfort index. This approach facilitates the construction of a comparative picture of the evolution of human thermal discomfort over a period exceeding a century, under changing climatic and urban conditions.

Thermal stress calendars were developed for Athens for the period 1901–2024, for each discomfort index (TDI, HMDX, HI), which are presented in Figure 3a–c. The horizontal axis represents calendar years and the vertical axis represents Julian days (1–365 or 366). Each cell corresponds to one day, while its color represents the level of thermal discomfort based on five defined categories: *green*: no discomfort (TDI < 21 °C, HMDX < 20 °C, HI < 27 °C); *blue*: little discomfort (21 ≤ TDI < 24 °C, 20 ≤ HMDX < 30 °C, 27 ≤ HI < 32 °C); *orange*: over 50% of the population feels discomfort (24 ≤ TDI < 27 °C, 30 ≤ HMDX < 38 °C,

32 ≤ HI < 41 °C); *red*: everyone feels severe stress: (27 ≤ TDI < 29 °C, 38 ≤ HMDX < 45 °C, 41 ≤ HI < 54 °C); and *purple*: extreme danger (TDI ≥ 29 °C, HMDX ≥ 45 °C, HI ≥ 54 °C). White boxes correspond to days for which no data was available (i.e., one or both of the input variables Ta or RH are missing), which did not affect the research, corresponding to less than 0.65% of input parameter availability for a period of 124 years.

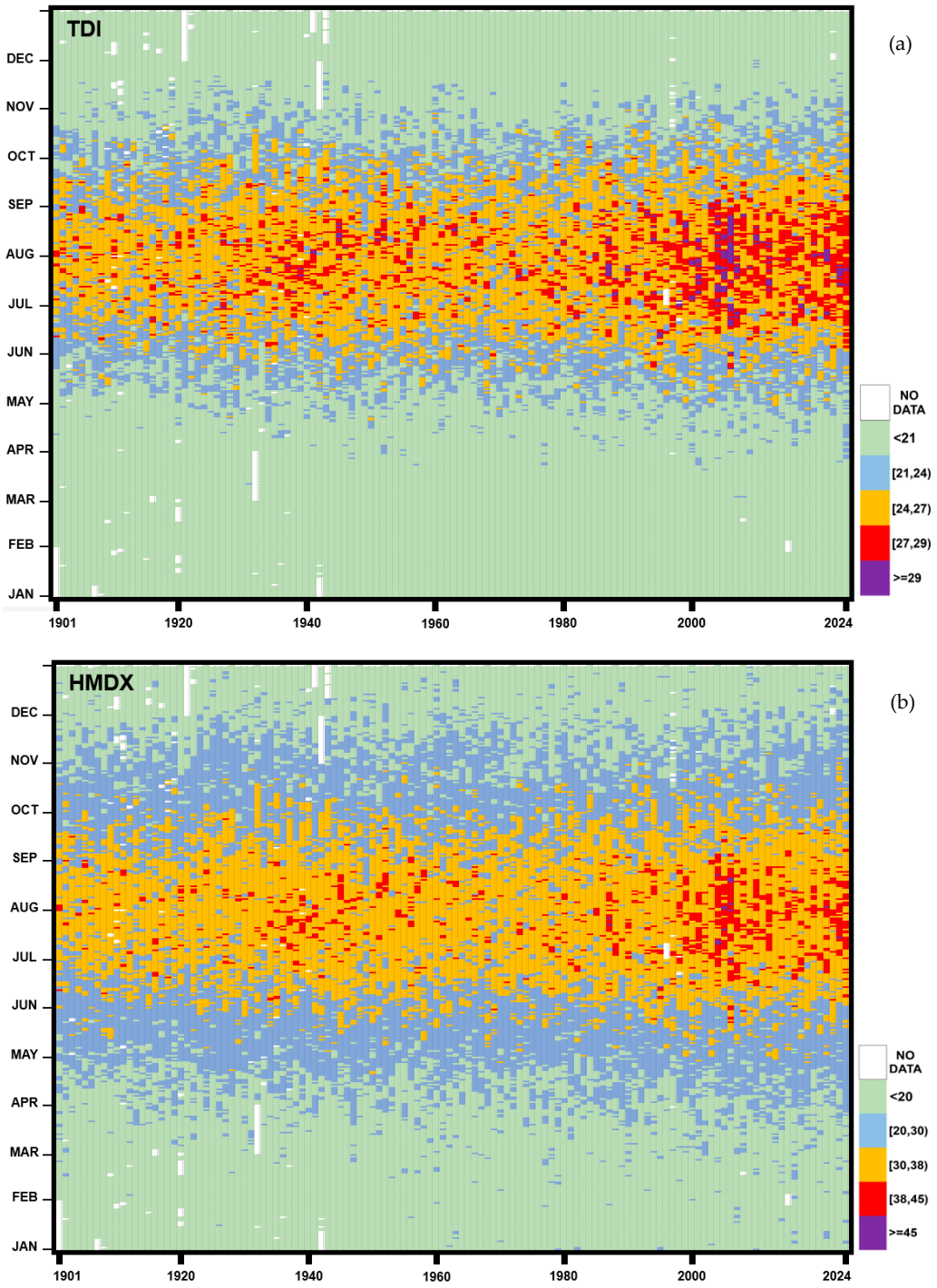

Figure 3. *Cont.*

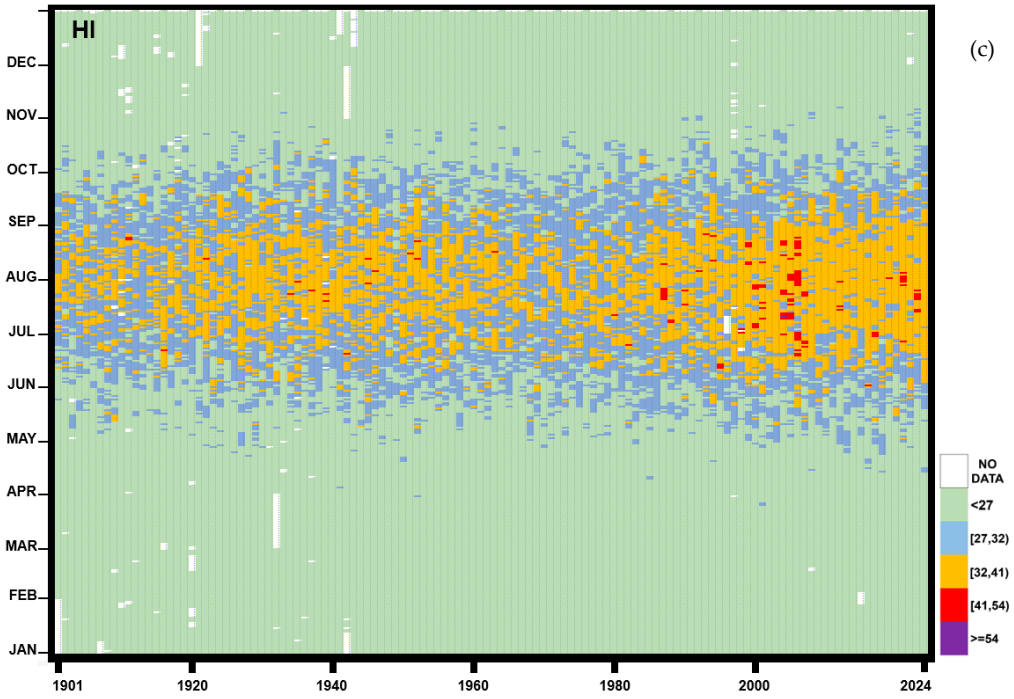

Figure 3. Calendar evolution of (**a**) Thom's Discomfort Index (TDI), (**b**) Humidex Index (HMDX) based on adjusted discomfort thresholds, and (**c**) Heat Index (HI), for Athens, Greece, for the examined period 1901–2024.

All three indices exhibit steady deterioration since 1980. The TDI (Figure 3a) shows an expanding discomfort core during July–August, with a rapid increase in days exceeding most of the population suffering discomfort and everyone feeling severe stress (red and purple). In the HMDX graph (Figure 3b), the orange zone (HMDX $\geq$ 30 °C) expands significantly after 1960 and, after 1990, covers almost the entire July–August period. The red cells (HMDX $\geq$ 38 °C) have gone from being rare to happening every year, while the first purple days ($\geq$45 °C) showed up in the mid-2000s, pointing to a new level of danger. Regarding the HI (Figure 3c), despite the higher "base" (discomfort when TDI $\geq$ 27 °C), the orange cells only become widespread after 1980. The HI $\geq$ 41 °C (red) risk category entered the climate "norm" after 2000. Despite threshold differences, all indices reveal a synchronized acceleration post-1980: the duration of thermal stress expanded and new "health emergency" classes emerged. Indices incorporating humidity (HMDX, HI) show stronger upward trends, confirming increases in relative humidity alongside warming.

The qualitative trend of the expansion of the period of great thermal discomfort, which is reflected in Figure 3a–c, is quantitatively confirmed in Figure 4. Figure 4b–d presents the day of the first and last appearances of the hazardous values of all three indices, i.e., TDI $\geq$ 27 °C, HMDX $\geq$ 38 °C, and HI $\geq$ 32 °C. Also, in the upper part of each sub-figure of Figure 4, the duration of the period between the first and last day is given as well, for each year.

Moreover, in order to quantify extreme heat events in Athens during the specified period (1901–2024), not necessarily during consecutives days, the 90th percentile of maximum temperature—a widely adopted metric in climatological studies—was implemented. The 90th percentile of temperature is more consistent across heat stress indices such as HI and HMDX in most operational contexts, as it encompasses a broader range of extreme events, aligning with public health warnings [96–102]. For each year between 1901 and 2024, the 90th percentile of daily maximum temperatures (Tmax) was determined. The mean of these values was then calculated, resulting in a critical value of 32.6 °C for the entire

period under review. In Figure 4a the day of the first and last appearance of the critical value Tmax $\geq$ 32.6 °C is presented.

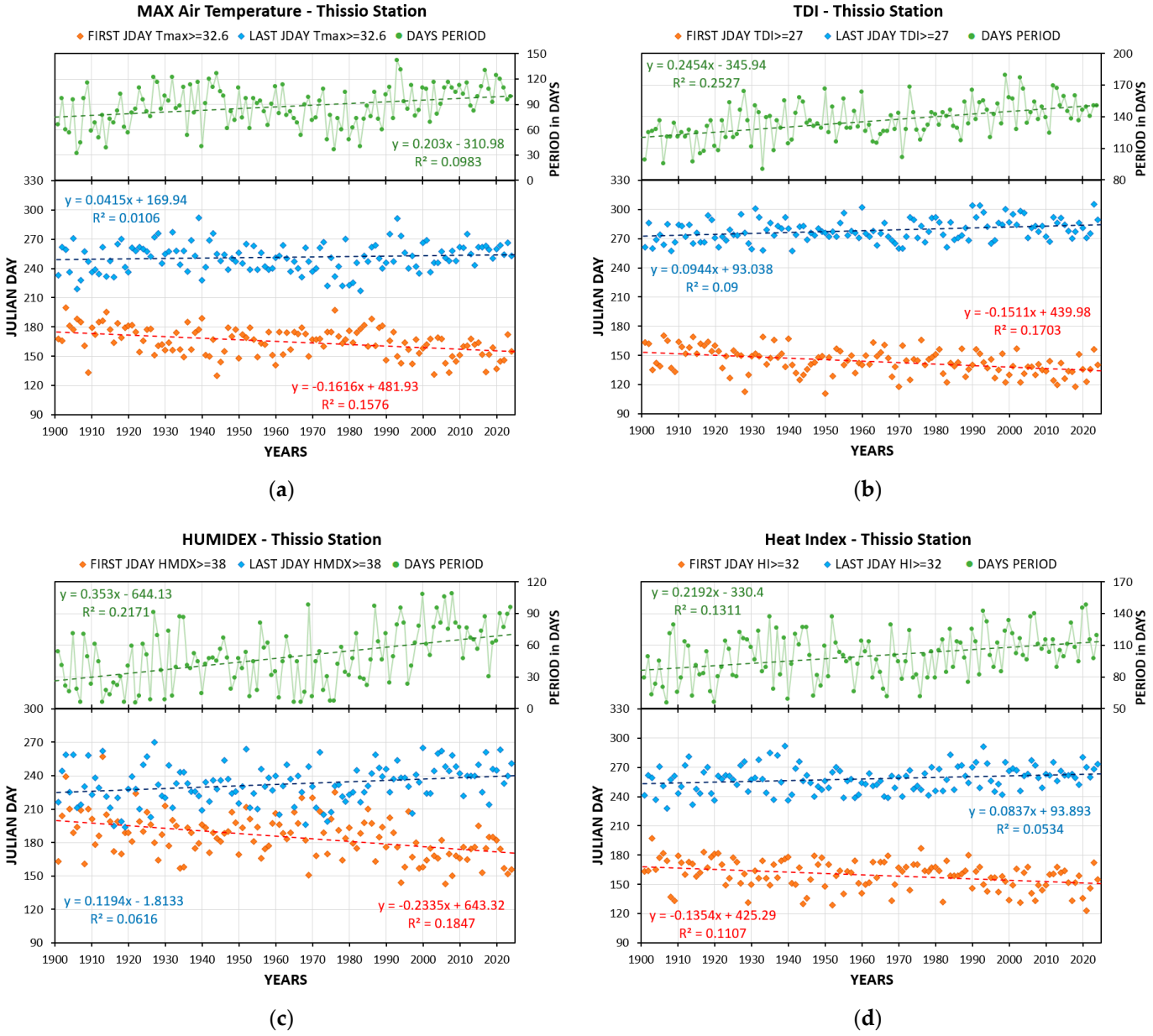

Figure 4. Temporal trends in the timing and duration of hazardous thermal conditions at the Thissio station in Athens, based on (**a**) Tmax $\geq$ 32.6 °C, (**b**) TDI $\geq$ 27 °C, (**c**) HMDX $\geq$ 38 °C, and (**d**) HI $\geq$ 32 °C. For each index, the lower panel displays the dates (Julian day) of the first (orange dots) and last (blue dots) occurrence of hazardous values, while the upper panel (green dots and lines) shows the annual length of the period (in days) between the first and last occurrence. Linear regression lines with R^2 values are also included (red, blue and green dashed lines).

According to the regression results, based on Tmax (Figure 4a), the first occurrence of such hot days within the year has been shifting progressively earlier, at a rate of 1.6 days per decade. This trend indicates that extreme temperature episodes tend to emerge earlier in the warm season, particularly since the late 20th century. On the other hand, the last annual occurrence is shifted later over the years by only 0.4 days per decade, a trend that is statistically weak. The overall duration of the period spanning from the first to the last appearance of such events increase over time, with a slightly increasing trend of 2 days

per decade, suggesting that extreme heat events, in addition to starting earlier, are steadily extending later in the year.

The corresponding shifts for the TDI (Figure 4b) are similar to those for Tmax regarding the first day and the last day within the year, where TDI's specific threshold (TDI $\geq$ 27 °C) is observed to be exceeded. The first occurrence of a day on which the majority of the population suffers discomfort shifts earlier by 1.5 days per decade, while the last occurrence shifts later by approximately 1 day per decade over the years, a trend which is not statistically significant. However, the total duration of the period from the first to the last occurrence of such events increases significantly over time, by approximately 2.5 days per decade. This increase is evident especially after the 1990s, when this has been observed systematically from June to September, while in some cases after 2000 it extends to October.

The results based on HMDX (Figure 4c) indicate that the shifts in the first and the last appearance of very strong heat stress (HMDX $\geq$ 38 °C) are more prominent than the shifts in the TDI. The first appearance tends to occur earlier, at a rate of 2.335 days per decade. The last appearance occurs later, at a rate of approximately 1.2 days per decade. The total period from the first to the last occurrence of such events lasts 3.53 days per decade. The progressive lengthening of the period of dangerous HMDX's values has been more intense in the last three decades (1991–2024), a period during which both the frequency and duration of these days have increased. The duration of this period is over 70 days per year on average, compared with around 40 days per year in the first half of the 20th century. Furthermore, after 2000, the period has exceeded 90 days in several years, indicating an accelerating trend.

The corresponding shifts for the HI (Figure 4d) are not as pronounced as those for HMDX and the slopes of the trend lines are not as steep as HMDX's. The first day with extreme caution (HI $\geq$ 32 °C) is shifted earlier by 1.4 days per decade, while the last occurrence is extended by 0.8 days per decade, a trend which is not statistically significant. However, although the rate of increase in duration is smaller compared with HMDX, a systematic extension of the period of intense discomfort is observed, with its duration increasing at a rate of 2.2 days per decade. This increase, as in the case of TDI, is particularly evident after the 1990s, when it is systematically observed from June to September, while in some cases after 2000 it extends until October.

3.2. Monthly Frequency of High Thermal Discomfort Days

For the purpose of investigating the appearance of outlier cases for TDI, HMDX, and HI indices, incorporating estimated values with a 1 h interval, the total number of days per month (not necessarily consecutives) where at least one hour of great to extreme discomfort (TDI $\geq$ 27 °C, HMDX $\geq$ 38 °C, HI $\geq$ 32 °C) appeared are introduced in Figure 5, for each year of the examined period 1901–2024. The results of our analysis are given in table format in Appendix C.

In the early decades of the 20th century, exceedances of TDI $\geq$ 27 °C and HMDX $\geq$ 38 °C were isolated and generally confined to the core summer months (July and August). Over time, and especially after the 1980s, the frequency and temporal distribution of threshold exceedances expand significantly. Especially after 2000, Figure 5 shows a notable increase in both the frequency and duration of conditions of increased TDI and HMDX, as the boxes show an increasingly intense red hue, indicating an increase in the number of days with intense discomfort. The increase in months outlined in black reflects the continuous presence of days with severe thermal discomfort. Almost every year in the 2010s and 2020s during summer show consistently more intense red shading and numerous black boxes, highlighting the existence of too many days, even entire months, with episodes of

severe thermal discomfort. It is worth noting that extreme exceedances of the thresholds (TDI $\geq$ 32 °C, HMDX $\geq$ 45 °C) were almost non-existent in the first half of the century, but have been occurring since 1980, even at the beginning of summer. Regarding the HI, by the 1990s, virtually every summer displayed up to 25 exceedance days during July and August, while in some years there were several days with HI $\geq$ 32 °C in June and September. The escalation in severity is emphasized by the increasing prevalence of months with days with HI $\geq$ 41 °C since the late 1980s, as well as by the first appearance of months with HI $\geq$ 54 °C. These findings demonstrate the increased heat stress attributed to both rising temperatures and increasing humidity, requiring targeted adaptations and public health interventions for Mediterranean urban areas.

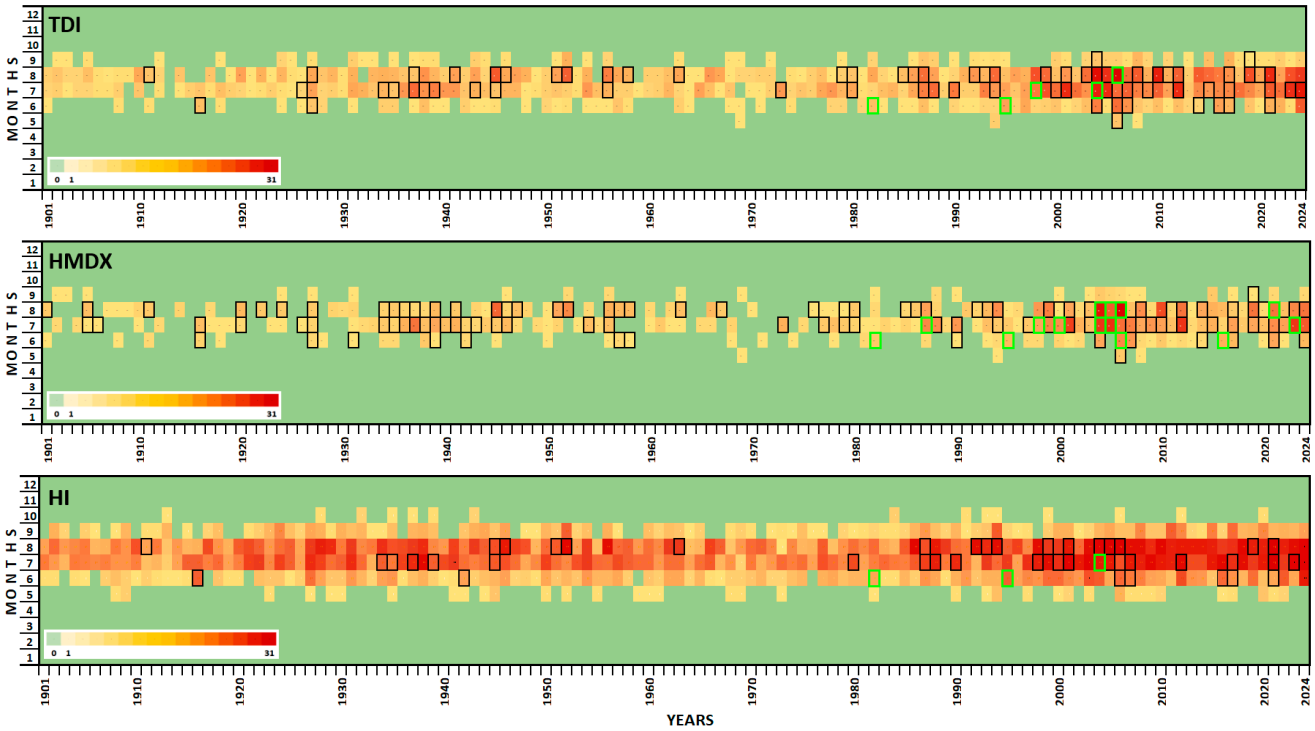

Figure 5. Number of days per month for each examined year where TDI values $\geq$ 27 °C (**up**), HMDX values $\geq$ 38 °C (**middle**), and HI values $\geq$ 32 °C (**down**) are observed. In black boxes, months also including days where values of TDI $\geq$ 29 °C (**up**), HMDX $\geq$ 40 °C (**middle**), and HI values $\geq$ 41 °C (**down**) are marked. In bright green boxes, months including days where extreme values of TDI $\geq$ 32 °C (up), HMDX $\geq$ 45 °C (**middle**), and HI $\geq$ 54 °C (**down**) are also marked. Months with zero days of occurrence are given with light green color.

3.3. Seasonal Distribution of Thermal Discomfort

In order to investigate in detail the hot season from June to August, including also the neighboring months, one before (May) and two after (September and October), available 1 h indices calculations are classified according to the categories in Tables 1–3, for 20-year intervals. The four-year period 2021–2024 has been included in the 2001–2020 period. The calculated percentage frequency per month and period was then normalized using the number of days per month (30 or 31) in order for the results to be expressed as number of days per class (not as %), for each index separately. The results for each index are presented in Figure 6a–c. Furthermore, Table 4 presents per index the total number of hours with high discomfort (TDI $\geq$ 27 °C, HMDX $\geq$ 38 °C, HI $\geq$ 32 °C), only from June to September, as most cases of thermal discomfort occur during these months. As can be easily seen, discomfort indices increase from June, peak in July and August, and decrease until October.

The analysis clearly shows an increase in thermal discomfort over a period of 20 years, especially after 1980, with the peak occurring after 2000. In the first decades of the 20th century, the overwhelming majority of summer days were recorded in categories of low (TDI < 21 °C, HMDX < 20 °C, HI < 27 °C) or moderate discomfort (21 ≤ TDI < 24 °C, 20 ≤ HMDX < 30 °C, 27 ≤ HI < 32 °C), while high discomfort categories were almost never observed. From 1941 to 1980, there was an increase of up to 34% of these days compared with previous years, with this growth rising to 38% in July and August alone, which are the most dangerous months. After the 1980s, the number of these days continued to increase gradually.

During the period 1981–2000, the days of the peak of summer, when more than half of the population felt discomfort, were almost as numerous as those days during the previous forty years. In the last two decades, these days have become more numerous than low-risk ones and have increased by more than 100% compared with the previous two decades. More specifically, the three discomfort indices show an increase in these days of 175%, 219%, and 112%, respectively, compared with the period 1981–2000. Also, looking at the TDI and HMDX charts (Figure 6a,b), it is clear that there are now more "dangerous" days, when everyone feels intense discomfort, indicating clear climate deterioration and increased heat stress conditions. This significant change reflects the growing impact of climate change, which has intensified the frequency, duration, and severity of heat waves in recent decades. The sharp increase in thermal discomfort indices corresponds to ob-served global warmings trends, highlighting the direct impact of climate change on ther-mal stress.

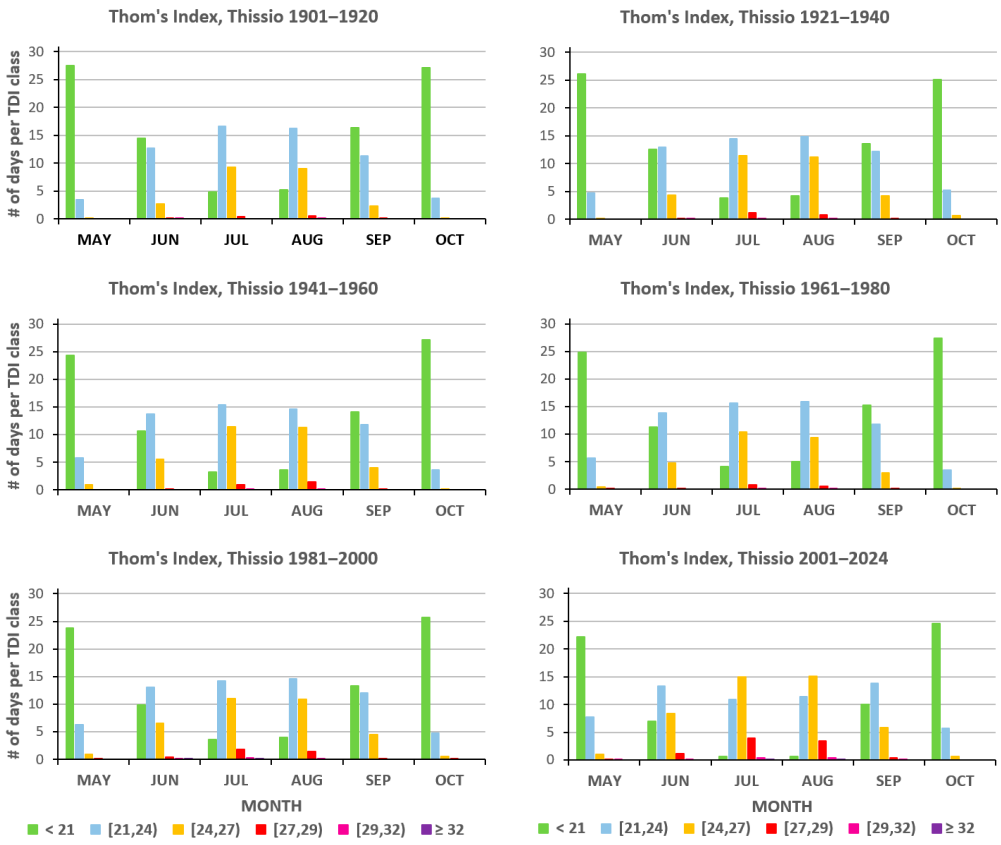

(**a**)

Figure 6. *Cont.*

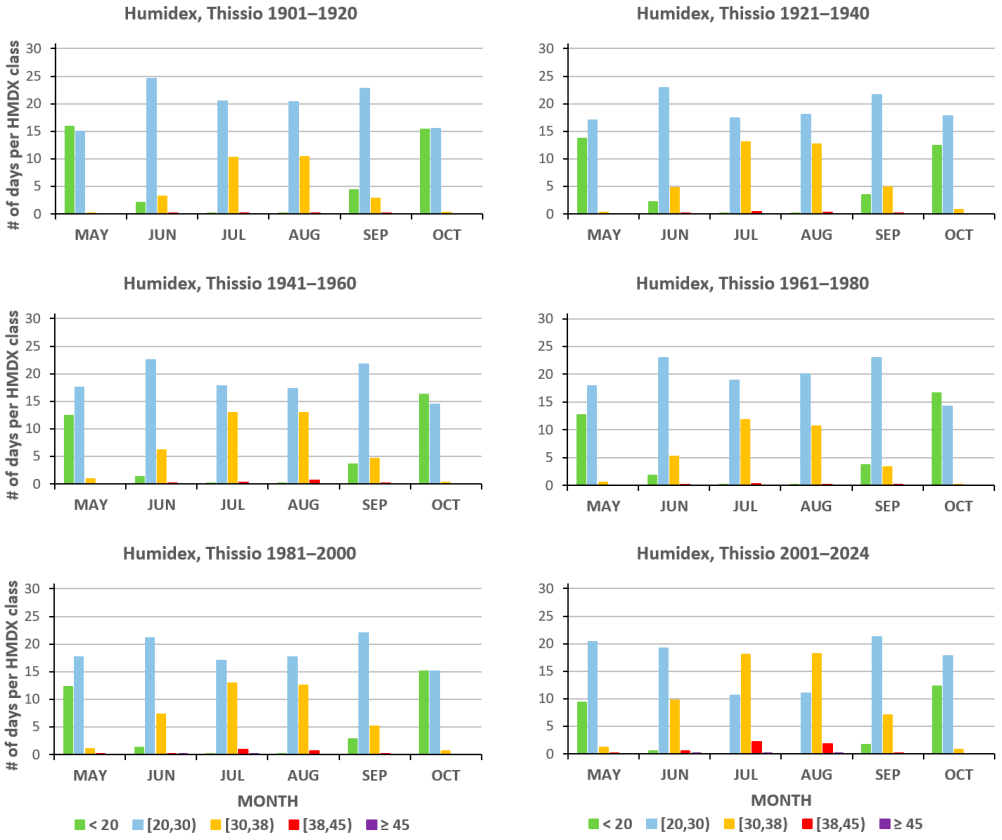

(**b**)

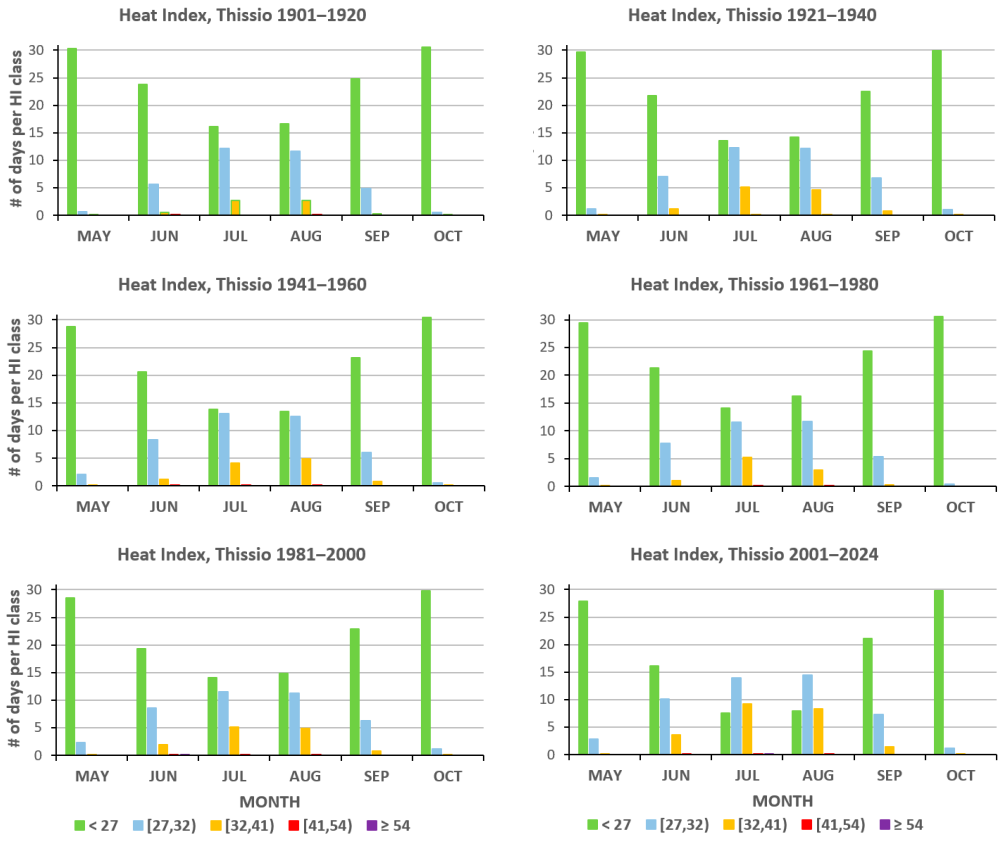

(**c**)

Figure 6. Monthly distribution of (**a**) TDI, (**b**) HMDX and (**c**) HI classes from May to October, in Athens, Greece, per 20-year intervals for the examined period 1901–2024. The four-year period 2021–2024 has been included into the 2001–2020 period.

Table 4. Total number of great discomfort hours from June to September in Athens, Greece, during the examined period 1901–2024, per 20-year intervals. The four-year period 2021–2024 has been included into the 2001–2020 period.

	Month	1901–1920	1921–1940	1941–1960	1961–1980	1981–2000	2001–2024
Number of hours where TDI $\geq$ 27 °C	JUN	54	82	91	41	242	746
	JUL	166	551	441	386	991	2534
	AUG	260	377	741	284	742	2224
	SEP	16	29	64	10	60	204
	Total	***496***	***1039***	***1337***	***721***	***2035***	***5708***
Number of hours where HMDX $\geq$ 38 °C	JUN	25	22	26	4	87	344
	JUL	54	198	145	117	431	1297
	AUG	95	119	305	75	314	1077
	SEP	3	5	15	2	8	53
	Total	***177***	***344***	***491***	***198***	***840***	***2771***
Number of hours where HI $\geq$ 32 °C	JUN	278	555	543	475	966	2138
	JUL	1267	2497	1988	1659	2520	5421
	AUG	1332	2212	2356	1441	2361	4951
	SEP	160	368	407	138	390	858
	Total	***3037***	***5632***	***5294***	***3713***	***6237***	***13,368***

3.4. Statistical Distribution of Meteorological and Discomfort Variables

In Figure 7, box and whisker plots incorporating all available 1 h values of the input parameters (Ta, RH) and calculated indices (TDI, HMDX, and HI) values are presented per decade and for the whole period 1901–2024. The four-year period 2021–2024 has been included in the 2011–2020 period. In Table 5, the main statistical values of the above parameters and indices but for the whole examined period 1901–2024 as a total are also given.

The interquartile range (IQR) of air temperature presents a gradual increase over the decades, starting from 11.4 in the first decade and rising to 12.1–12.5 in the last. This corresponds to an overall increase from 6.14% to 9.65%, suggesting that the intermediate temperatures (between 25th and 75th percentiles) are increasingly different. The distance between the adjusted trend lines shows a steady mean increase of 0.78% per decade, reflecting a gradual but steady increase in variability.

The IQR variation over time for relative humidity shows a significant decrease over the examined period. From 29.0 in the first decade, it falls to 24.0 in the last, recording a decrease of 17.24%. The linear regression confirms a steady downwards trend at a rate of −1.25% per decade. This trend reveals that the intermediate values of relative humidity converge to a smaller range, which may reflect the prevalence of drier and more stable conditions, possibly due to the impact of climatic change on the hydrological cycle. The IQR of the TDI starts at 8.7, reaches 9.7 during the decade of 1991–2000, and drops to 9.0 during the last decade. This increase shows that TDI values have a greater dispersion over the decades. This implies that the range of discomfort is widening, and possibly more days are reaching values closer to thresholds of severe discomfort. The regression values demonstrate a steady mean increase in IQR at a rate of +0.74% per decade, confirming the increasing trend. The IQR variation over time for HMDX reveals a clear trend of increasing intra-decadal variance. HMDX shows an overall increase in IQR as high as 14.94% from 1991 to 2010, with a constant rate of +0.96% per decade. These rises suggest that thermal discomfort conditions are becoming increasingly unstable. The HI exhibits the most significant rise in IQR, increasing from 11.4 during the first decade to 12.8 in the last, an increase of 12.8%. The linear regression confirms an upward trend at a rate of +1.03%

per decade. This marked change indicates that the variability of thermal stress is rapidly increasing, causing increasingly unpredictable discomfort conditions. The widening of the mean values reinforces the need to adopt adaptation strategies to ensure the protection of public health.

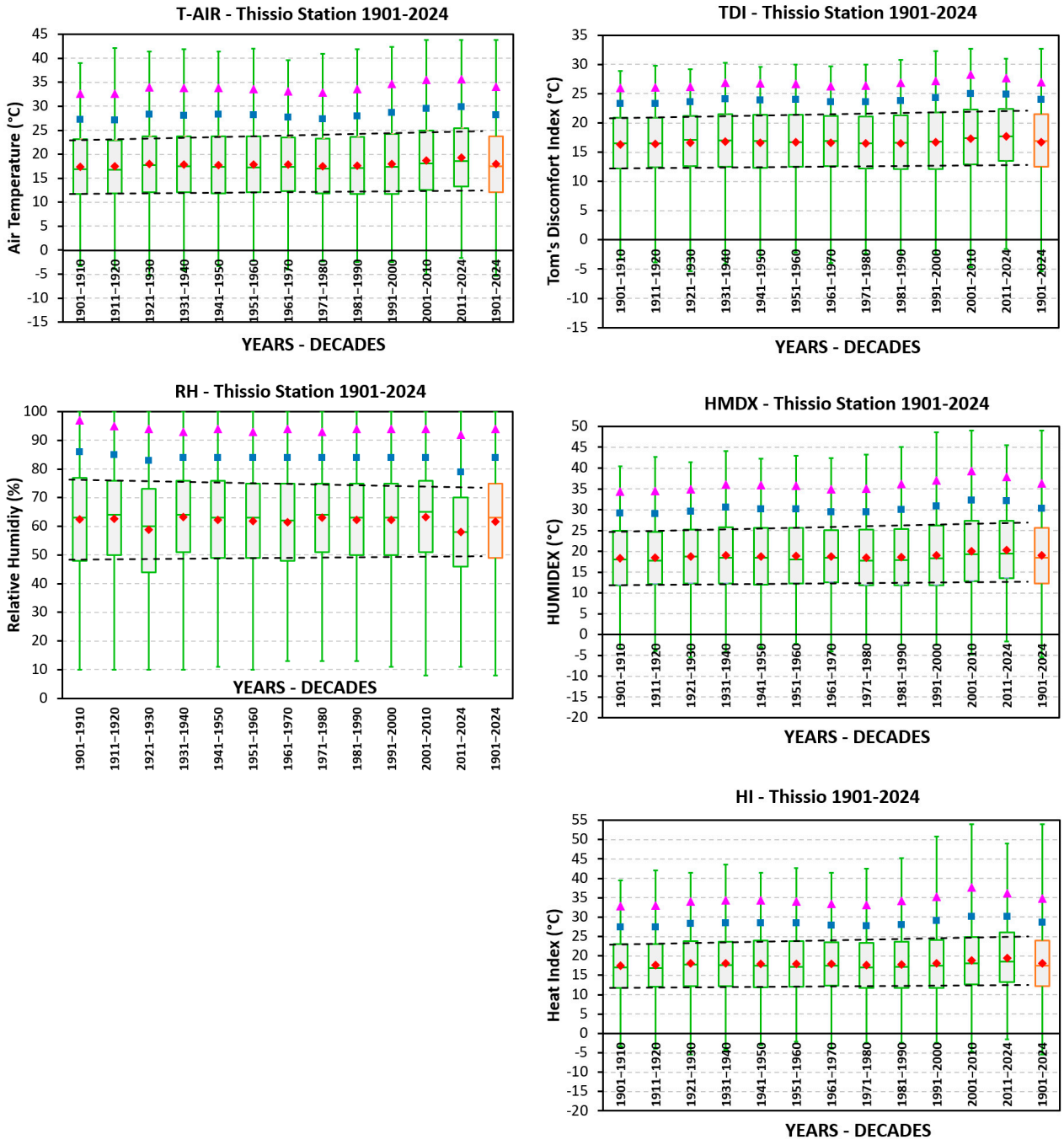

Figure 7. Box and whisker plots of air temperature, relative humidity, TDI, HMDX, and HI hourly values for the period 1901–2024, in 10-year intervals (green boxes) and for the whole period (red boxes), presenting 25% (Q1) and 75% (Q3) percentiles, median (red diamonds), and average (green lines) values, and max–min outliers. Also, both 90th (blue squares) and 99th (magenta tringles) percentiles are presented. Linear trends (dash lines) at each quartile (25% and 75%) of all parameters examined are also included.

Table 5. Main statistical values for each parameter, for the examined period 1901–2024, for Athens.

Statistical Parameter	Ta	RH	TDI	HMDX	HI
Number of values	1,083,876	1,082,598	1,079,938	1,079,938	1,079,938
Average	17.97	61.6	16.76	19.00	18.09
Standard deviation	7.57	17.1	5.69	8.35	7.70
Minimum	−5.4	8	−5.4	−5.4	−5.4
1st Quartile (25%)	12.1	49	12.5	12.3	12.2
Median (50%)	17.5	63	16.9	18.4	17.5
3rd Quartile (75%)	23.8	75	21.5	25.7	23.9
Maximum	43.8	100	32.7	49.0	54.0
90th Percentile	28.2	84	24.0	30.3	28.6
99th Percentile	34.1	94	27.0	36.4	34.8

A progressive and statistically meaningful increase in both the median and maximum values is clearly evident from the 1980s, reflecting a marked intensification of thermal discomfort over time. Specifically, while the median TDI values remained relatively stable, between 16.5 °C and 17 °C, from 1901 to 1980, a significant upward trend occurred in the last decade, when the median rose to ≈18 °C. This shift indicates that typical summer thermal conditions are no longer confined to moderate discomfort levels but are transitioning towards more intense bioclimatic stress for the general population. The observed rise in TDI median values is mirrored by a concurrent increase in maximum values, which reaches nearly 35 °C in the decades of 1981–1990 and 2001–2010, which is significantly higher than those recorded in earlier periods. These elevated maximum values are accompanied by the higher interquartile ranges and upper whisker extensions, indicating a growing occurrence of high-discomfort events. Even more pronounced trends are identified for the HMDX and HI statistics. While the median HMDX and HI values increased from ≈18 °C and ≈17 °C (1901–1930) to 19.3 °C and 18.4 °C accordingly in the 2011–2024 period, the mean values rose from 18.3 °C and 17.5 °C to over 20 °C and 19 °C in the same time frame, highlighting a systemic shift towards more oppressive summer conditions across the entire distribution. Most critically, the maximum values of HMDX and HI rose dramatically, peaking at 49 °C and 54 °C during the 2001–2010 decade. These values are not only exceptionally high, but surpass the well-established danger thresholds, above which heat-related health effects such as heat exhaustion or even heat stroke become a serious concern. This finding underscores the growing public health implications of climate change, especially for vulnerable populations.

The evolution of the TDI, HMDX, and HI over the 20th and early 21st centuries reveals not only a clear warming trend but also a transition towards more frequent and intense thermal discomfort conditions. The need for adaptive urban planning and targeted public health strategies is underscored by these trends in response to rising heat stress, especially in densely populated urban environments like Athens.

3.5. Decadal Classification of Thermal Discomfort Conditions

In order to illustrate the decadal distribution of the number of days per year falling into different thermal discomfort categories, the daily maximum values of each index were employed once again for the days' characterization. The four-year period 2021–2024 has been included in the 2011–2020 period. In Figure 8a–c (left column), each vertical bar represents the average number of days per decade in specific discomfort ranges, expressed as the percentage (%) of the total days available in each decade. In order for more details to be revealed in Figure 8a–c, a magnification of the top 2–3% was provided for each index (extreme classes). These three figures provide information on the temporal evolution of

thermal stress levels observed in Athens from 1901 to 2024, reflecting both the frequency and severity of thermal stress over time.

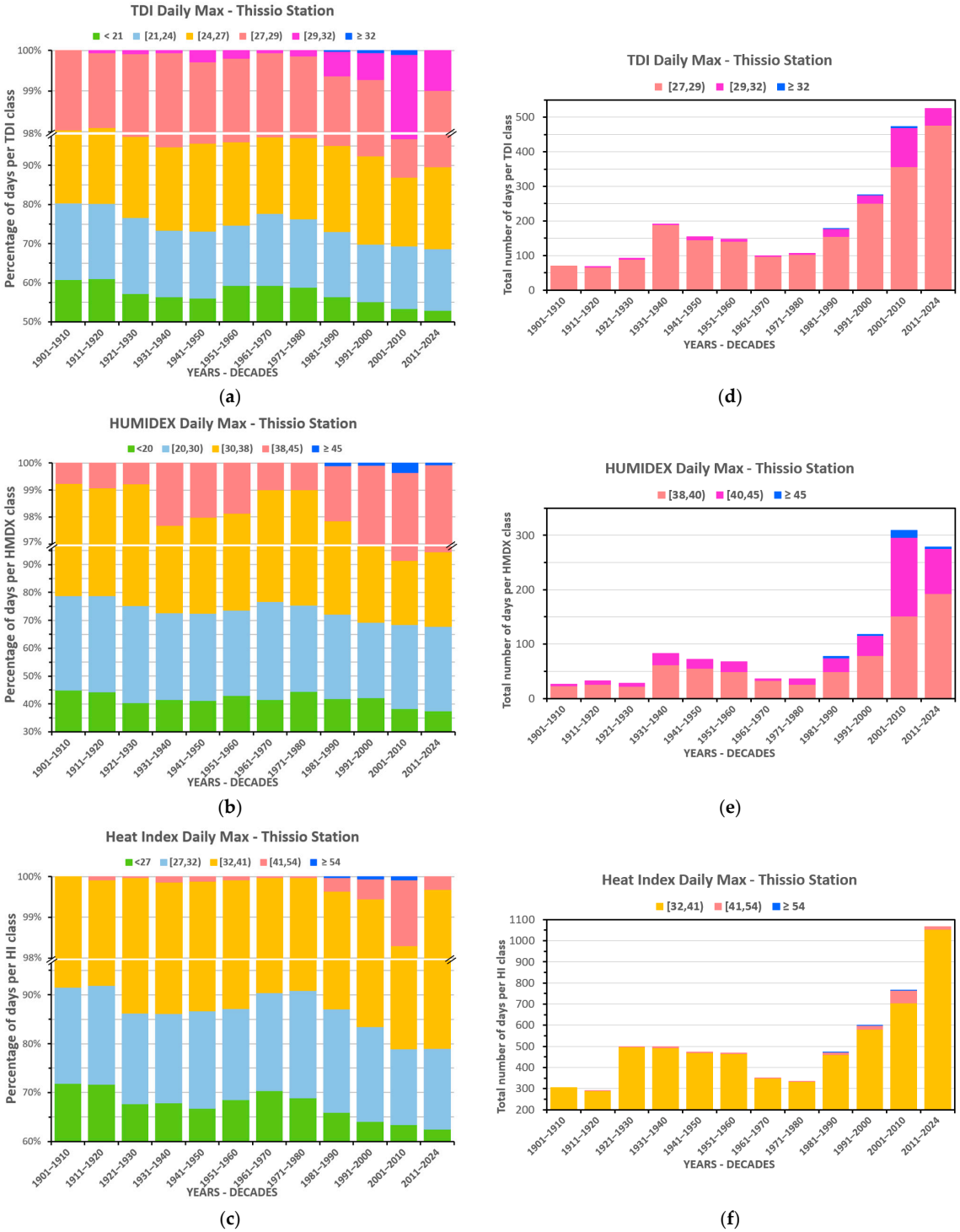

Figure 8. Decadal distribution of thermal discomfort conditions in Athens during the 1901–2024 period, based on the daily maximum values of the TDI (**a**,**d**), HMDX (**b**,**e**), and HI (**c**,**f**). In (**a**–**c**), each bar represents the total number of days per decade that fall within specific discomfort classes, expressed as percentage of days available in each decade.

For the TDI (Figure 8a) and from 1951 to 1980, the frequency of days on which more than half of the population felt discomfort ($24 \leq$ TDI < 27 °C) and the majority of the population suffered discomfort ($27 \leq$ TDI < 29 °C) began to increase, with the majority of

the population beginning to experience significant thermal discomfort compared with the early decades. An even more pronounced change occurred after 1980, especially during the decades 2001–2010 and 2011–2020, when the number of days on which most of the population suffered discomfort more than doubled, and for the first time there were days when emergency medical assistance was required (TDI $\geq$ 32 °C).

A similar trend is observed in the distribution of the HMDX (Figure 8b) and HI (Figure 8c) indices. During the first half of the 20th century, the majority of summer days have taken values of HMDX < 30 °C and HI < 32 °C, and consequently, especially in the categories for HMDX < 20 °C and HI < 27 °C, days are not characterized as discomfort days. Since the 1950s, there has been a decrease in the number of discomfort-free days, according to the HMDX and HI indices, and an increase in the number of days classified as "some discomfort", which represents a certain level of discomfort that makes it necessary to limit physical activity. HMDX analysis shows that days indicating dangerous levels of discomfort have been steadily increasing since 1980 and have doubled in recent decades. The most extreme category of HMDX—and the days when, according to HI, heatstroke is likely—first appeared after 1980. This development highlights the transition from thermally safe to increasingly dangerous conditions, reinforcing the role of humidity in amplifying the risk from heat.

Complementary to Figure 8a–c, Figure 8d–f (right column) present more details on the distribution of great discomfort days in Athens during the period under study. More specifically, it depicts the total number of days whose daily maximum falls within the highest discomfort classes of each index per decade (TDI $\geq$ 27 °C, HMDX $\geq$ 38 °C, HI $\geq$ 32 °C). The first notable increase in discomfort days is observed in the decade 1931–1940, when days of high discomfort almost doubled compared with previous decades, adding on average one more day per decade of severe discomfort observed (see Figure A1 given in Appendix D, where the % increase is expressed in equivalent number of days per decade).

A rapid change occurs after the 1980s. The peak is at the beginning of the 21st century, when the number of days on which the majority of the population suffers from discomfort almost sextupled compared with the first decades of the 20th century. Based on the average of all three indices, during the decade 2001–2010, around 4 days per decade of severe thermal discomfort are identified, followed by the next period 2011–2024 where the number of these days found to be 3.8 per decade. This increase is noteworthy because, until the 1971–1980 decade, no more than two such days per decade were observed.

In addition, days with health hazards are becoming more frequent: from sporadic occurrences to more than 100 days in the decade 2001–2010, marking a shift from occasional dangerous episodes of thermal discomfort to recurring phenomena with implications for public health. The three graphs show (Figure 8d–f) not only the clear transition to more severe conditions of thermal discomfort, but also the increase in the number of days that exceed dangerous levels of thermal stress, emphasizing the intensification of thermal risk in recent decades.

4. Discussion

The present analysis, based on more than a century (1901–2024) of hourly meteorological observations of Athens, underlines a marked and accelerating increase in thermal discomfort, as expressed by three simple but widely used indices (TDI, HMDX, HI). The results indicate that both the frequency and intensity of heat stress conditions have increased significantly over the last four decades, with the most dramatic increase occurring after 2000. This pattern is consistent with the broader phenomenon of warming in the eastern Mediterranean but is further amplified by local urban dynamics. The intensification is

clearly reflected in the graphical analyses, which provide complementary perspectives on daily, monthly, seasonal, and decadal patterns.

Daily calendar analyses emphasize the progressive expansion of the core of discomfort since the mid-20th century. While in the early decades, days of high discomfort were sporadic and limited to July and August, after 1980 they became systematic and extended to June through September, and occasionally into October. Extreme categories (TDI $\geq$ 32 °C, HMDX $\geq$ 45 °C, HI $\geq$ 54 °C), which were almost non-existent before 1980, have appeared in the last two decades. This extension of the dangerous period is consistent with earlier reports of a delayed summer temperature increase in the eastern Mediterranean until the 1980s [83] and the subsequent sharp increase in average summer temperatures in Athens [84].

The total duration of the hazardous period now exceeds 90 days in some years, compared with less than 40 days in the early 20th century. These results corroborate Katavoutas and Founda [68], who found an increasing risk of heat stress in Athens during 1960–2017, and extend their findings by demonstrating that the acceleration is strongest after 2000.

The monthly and seasonal decadal averages reveal a structural upward shift of ≈3 °C across all indices between 1901 and 1940 and 2001–2024. Particularly noteworthy is the rise in September values, confirming that the thermal stress season now extends into early autumn. These findings support earlier work by Bartzokas et al. [63], who reported an intensification of intra-annual discomfort variability, and by Pantavou et al. [66,67], who identified prolonged periods of elevated heat stress in Athens.

The classification of discomfort categories by month further emphasizes this expansion. While in 1901–1940, almost all summer days fell within the low - to moderate - discomfort classes, after 2000 more than 100% increases are observed in severe categories compared with 1981–2000. The cumulative hours of high discomfort rose from ≈500–700 h in 1901–1920 to over 13,000 h in 2001–2024 for HI $\geq$ 32 °C, a nearly 20-fold increase. These results extend the findings by Paliatsos and Nastos [61], who linked high TDI values to pollution episodes in the summers of 1993–1995 by showing that such discomfort is no longer tied to episodic conditions but dominates the warm season climatology.

Statistical distributions demonstrate both rising central tendencies and widening variability. These findings are in agreement with Stathopoulou et al. [36], who mapped high TDI values from satellite observations in the 1990s, but the present analysis shows that both the frequency and variability of dangerous conditions have sharply escalated since then.

Finally, the decadal classification of daily maxima shows that the number of severe discomfort days sextupled after the 1980s and, in the decade 2001–2010, over 100 days per decade reached hazardous categories. This confirms the findings of Nastos and Matzarakis [64], who linked high PET/UTCI values to increased mortality in Athens in the 1990s by showing that the underlying climate has shifted into a regime of the persistent annual recurrence of such dangerous days.

Taken together, the graphical evidence demonstrates that Athens has undergone a transition from sporadic extreme heat events to a chronic regime of extended, frequent, and severe thermal discomfort. This transition is amplified by urbanization and the urban heat island effect, as noted in earlier works [63,68], and is consistent with broader Mediterranean and global trends [10,47,65]. The implications for public health, urban sustainability, and economic activity are severe. The observed trends highlight the need for integrated adaptation strategies, combining urban greening, heat warning systems, and the targeted protection of vulnerable populations.

5. Conclusions

The present study, which is based on 124 years (1901–2024) of high-resolution hourly meteorological records from the Thissio station in central Athens, Greece, demonstrates a significant and accelerating increase in thermal discomfort conditions during the 20th and early 21st centuries. A comprehensive analysis of the widely used bioclimatic indices, TDI, HMDX, and HI, reveals a pronounced trend toward more intense and protracted heat stress episodes since the 1980s, with the strongest acceleration occurring after 2000. Discomfort values that were once considered extreme are now common, occurring earlier in the summer and later in the autumn, extending the period of heat stress from June to September. The mean values, interquartile ranges, and maximum values of all indices exceed the thresholds associated with serious health risks, underscoring the combined impact of rising air temperatures, increasing humidity, and rapid urbanization on heat risk. However, this study is not without its limitations. The analysis is based on a single historical station, which is highly reliable with a long measurement record. However, it may not fully represent microclimatic variability across different urban landscapes in Athens. Furthermore, the selection of relatively simple indices facilitates long-term comparability; however, it does not capture the complete physiological complexity provided by more sophisticated indices. Future research should expand the spatial coverage by incorporating data from multiple stations or satellites, as well as information on land use and socioeconomic conditions. Moreover, it should also link meteorological trends directly to health records in order to better quantify heat-related risks. Such measures would enhance the process of evidence-based decision-making for sustainable and climate-resilient Mediterranean cities.

Author Contributions: Conceptualization, B.E.P.; methodology, B.E.P. and C.G.; data collection and quality control, B.E.P.; necessary software code development, B.E.P. and N.G.; analysis, investigation, and visualization, B.E.P. and N.G.; writing—original draft preparation, B.E.P. and N.G.; writing—review and editing, B.E.P., N.G. and C.G.; supervision, B.E.P.; funding acquisition, B.E.P. All authors have read and agreed to the published version of the manuscript.

Funding: This research was funded by the project "CLIMPACT II: Support for the upgrading of the National Research Network for Climate Change and Its Effects" (2023NA11900001, OPS 5201588), financed by the National Component of the Public Investment Program, National Development Program 2021–2025, Ministry of Development, General Secretariat for Research and Innovation.

Institutional Review Board Statement: Not applicable.

Informed Consent Statement: Not applicable.

Data Availability Statement: The datasets generated during the current study are available from the corresponding author upon reasonable request. Part of the analysis results are given freely in table form in Appendix C.

Acknowledgments: The authors of this article would like to thank all the anonymous observers who served at NOA's meteorological station in Thissio for their dedication in the day-by-day collection of all necessary measurements/observations and their careful processing/archiving, especially under very adverse conditions, often with the risk of their lives during times of war (World War II, Greek Civil War, etc.). The first author of this article wishes to express his personal gratitude to S. Lykoudis, D. Papagiannis, and V. Mitsopoulos for their invaluable assistance during the inaugural automation attempt of the Thissio meteorological station in 1995. Finally, the authors of this article would also like to thank all three anonymous reviewers for the valuable time they devoted to reading and commenting on this manuscript, thereby resulting in its improvement.

Conflicts of Interest: The authors declare no conflicts of interest.

Abbreviations

The following abbreviations are used in this manuscript:

TDI	Thom's Discomfort Index
HMDX	Humidex Discomfort Index
HI	Heat Index
UTCI	Universal Thermal Climate Index
WBGT	Wet-Bulb Globe Temperature
PET	Physiologically Equivalent Temperature
PMV	Predicted Mean Vote
IRQ	Interquartile Range
Ta	Air Temperature in °C
Tmax	Daily Maximum Air Temperature
RH	Air Relative Humidity in %
e	Vapor Pressure in hPa
TMY	Typical Meteorological Year
TMM	Typical Meteorological Month

Appendix A

The National Observatory of Athens (NOA) is the first research institution created in Greece (on 26 June 1842, during a solar eclipse) after its liberation from the Ottoman Empire (1828), the arrival of King Otto as the head of the modern Greek Kingdom (1833), and the establishment of Athens as the capital of the modern Greek state (1834). The hill of the Nymphs, selected as the place to build the Observatory, is one of the seven hills of Athens, a sanctuary of the Nymphs in antiquity, next to the Pnyka hill.

NOA's meteorological activities began in early 1858 with the systematic collection of daily observations in central Athens, but it was not until 1890 that a first-class meteorological station was permanently installed in Thissio, being in continuous operation ever since. According to the World Meteorological Organization's guidelines [69–71], the most important requirements for meteorological instruments to equip an observation station are reliability, accuracy, the simplicity of design, the convenience of operation and maintenance, and the strength of construction.

The psychrometric method was adopted at Thissio station to record the two basic parameters, temperature and humidity, that characterize atmospheric air, incorporating a pair of identical high-precision liquid-in-glass mercury thermometers, the dry- and the wet-bulb thermometers, with preferable scale intervals of 0.2 °C, having approximately the same lag coefficient. It is considered that the lag coefficient, defined as the time required by the thermometer to respond to 63% of a sudden change in temperature, should be between 30 and 60 s in a wind speed of 5 m/s. Thermometers for psychrometry should be accompanied with a factory correction certificate providing corrections, with an accuracy of ±0.1 °C, for at least six points spaced evenly across the range.

In addition, the set of psychrometric thermometers is accompanied by high-precision maximum and minimum thermometers, with scale intervals of 0.2 °C, for obtaining the required daily extreme observations. The maximum or Negretti thermometer is a mercury-in-glass thermometer, with a constriction in the bore below the lowest graduation, permitting its resetting without undue effort; however this prevents the mercury column from receding with falling temperature. The minimum or Rutherford thermometer is a spirit-in-glass (ethyl alcohol) thermometer, with a dark glass index (about 2 cm long) immersed in the spirit. Both maximum and minimum thermometers are supported nearly horizontally.

A wooden louvered Stevenson screen, with a volume of one cubic meter and natural ventilation, is used for all thermometers to be installed inside, protected from radiation from the Sun, sky, Earth, and any surrounding objects (i.e., large buildings and expanses of

concrete or tarmac), but at the same time be adequately ventilated for measurements to be representative of the free air circulating in the locality. The screen should be mounted at such a height that thermometer bulbs are between 1.25 and 2.0 m above the ground. Observations for synoptic purposes are taken on a daily basis at 08:00, 14:00, and 20:00 LST (Local Standard Time, LST = GMT + 2 h), with an allowed tolerance of 10 min before or after the synoptic hour. Thermometers should be read to the nearest 0.1 degree.

In order to cover the rest of the day with measurements in 1 h intervals, following standard practice, a pair of self-recording instruments was placed inside the meteorological screen: a bimetallic thermograph and a hair hygrograph. Both of them incorporate a sensing element and a form of rotating chart mechanism. A typical thermograph in good condition has a small lag coefficient of about 25–30 s in wind of 5m/sec, with a maximum error not exceeding 1 °C at any point of the range. On the other hand, for air temperatures between 0 and 30 °C and relative humidity between 20 and 80%, an hygrograph in good condition subjected to a sudden change in relative humidity indicates 90% of the change within about 3 min, to an accuracy within ±3%.

Paper thermo- and hygro-charts are subject to change once a week, during the observational time of 08:00 LST on Monday morning, and are read by station staff at 1 h intervals. Using the three synoptic observations available per day (08:00, 14:00, 20:00 LST), errors in the chart readings are evenly distributed using a linear interpolation technique and temperature and humidity measurements are finally corrected and stored in NOA's archives. These are the "true" 24-hourly values produced according to Professor Eginitis [72], who served as NOA's director for the period 1890–1934, organizing meteorological observations in NOA and establishing the first network of meteorological stations throughout the country.

In June 1995, the first attempt for automating the Thissio historical station was made by introducing inside the meteorological screen two high-precision platinum Pt100 thermometers (electrical thermometers with resistance close to 100 Ohm at 0 °C), in a shiny stainless steel outer case with a small diameter, with a nominal accuracy of less than ±0.2 °C and connected to a digital recorder (four-wire connection on a CR-21X datalogger, Campbell Scientific Ltd., Logan, UT, U.S.A.) to measure dry- and wet-bulb temperatures alongside with the traditional liquid-in-glass mercury thermometers.

The station's new digital files consist of one-minute averages of 15 s samples of both dry and wet temperatures, allowing the psychrometric method to be applied, estimating a number of humidity parameters at the same time step (relative humidity included). After an extensive comparison from April 1999 to February 2004, the bias between conventional and new instruments was estimated and monthly coefficients were developed and published [73]. The homogeneity at NOA's temperature time series was restored by eliminating the bias caused from the 1995 instrument change.

The availability of digital files with high temporal resolution (1 min time step) renders the process of reading and correcting paper charts redundant. The extraction of instantaneous measurements at specific times (e.g., 10:00, 11:00, or 12:00 LST) from digital files is now a straightforward process. Even so, the two autographic instruments, which were replaced in 2005 by a new combined thermo–hygrograph, continue to be located within the meteorological screen in order to serve as a backup in emergency situations involving extensive power failures.

In May 2017, according to a list of criteria, Thissio station was recognized by the World Meteorological Organization (WMO) as a long-term observing station for its high-quality climate records (WMO Decision 8, EC-69, May 2017).

Appendix B

Table A1. Population of the Greater Athens metropolitan area since the middle of the 19th century.

Year	Population	Notes
1834	~4000	Capital moved to Athens
1870	~44,500	Beginning of urban development
1896	~123,000	Year of the first modern Olympic Games
1921	~473,000	Before the Asia Minor Catastrophe
1928	~801,622	Large influx due to refugee crisis
1940	~1,124,000	Pre-war growth
1951	~1,379,000	Post-war reconstruction
1961	~1,853,000	Industrial development
1971	~2,541,000	Urban peak
1981	~2,969,000	Expansion of suburbs
1991	~3,444,000	Gradual stabilization
2001	~3,761,000	Post-Olympic infrastructure era
2011	~3,638,000	Start of demographic decline
2021	~3,744,059	Slight recovery, stabilization

Data sources: [78–82].

Appendix C

Table A2. Number of high discomfort hours and days (not necessarily consecutives), from May to October, for Athens, Greece, during the examined period 1901–2024 according to TDI, HMDX and HI indices.

Year	Month	TDI [27,29)		TDI [29,32)		TDI ≥ 32		HMDX [38,40)		HMDX [40,45)		HMDX ≥ 45		HI [32,44)		HI [41,54)		HI ≥ 54	
		Total Hours	Days	Total Hours	Days	Total Hours	Days	Total Hours	Days	Total Hours	Days	Total Hours	Days	Total Hours	Days	Total Hours	Days	Total Hours	Days
1901	MAY																		
	JUN	1	1					1	1					5	2				
	JUL	5	3											73	15				
	AUG	34	4					20	3	1	1			56	10				
	SEPT																		
	OCT																		
1902	MAY																		
	JUN													2	2				
	JUL	12	4					4	2					67	11				
	AUG	6	5											95	17				
	SEPT	5	1					1	1					27	8				
	OCT																		
1903	MAY																		
	JUN																		
	JUL	1	1											38	7				
	AUG	5	3											65	11				
	SEPT	1	1					1	1					13					
	OCT																		
1904	MAY																		
	JUN													6	2				
	JUL	8	3					2	2					71	15				
	AUG	5	3											80	13				
	SEPT																		
	OCT																		

Table A2. *Cont.*

Year	Month	TDI [27,29)		TDI [29,32)		TDI ≥ 32		HMDX [38,40)		HMDX [40,45)		HMDX ≥ 45		HI [32,44)		HI [41,54)		HI ≥ 54	
		Total Hours	Days	Total Hours	Days	Total Hours	Days	Total Hours	Days	Total Hours	Days	Total Hours	Days	Total Hours	Days	Total Hours	Days	Total Hours	Days
1905	MAY																		
	JUN													1	1				
	JUL	7	3					2	1	1	1			60	14				
	AUG	36	6					15	4	1	1			116	15				
	SEPT	8	2					1	1					21	4				
	OCT																		
1906	MAY																		
	JUN																		
	JUL	3	2							1	1			44	13				
	AUG	3	2											25	7				
	SEPT													1	1				
	OCT																		
1907	MAY																		
	JUN													7	4				
	JUL	2	2											62	14				
	AUG	2	1					1	1					51	8				
	SEPT																		
	OCT																		
1908	MAY													3	2				
	JUN	7	2					1	1					34	6				
	JUL	11	4											47	12				
	AUG	9	2					2	1					76	15				
	SEPT													5	1				
	OCT																		
1909	MAY													9	4				
	JUN													11	4				
	JUL													91	12				
	AUG	5	2					1	1					49	12				
	SEPT													15	7				
	OCT																		
1910	MAY																		
	JUN													7	1				
	JUL	21	5					2	1					70	14				
	AUG	24	9					3	3					97	20				
	SEPT																		
	OCT																		
1911	MAY							4	2										
	JUN	9	2											29	4				
	JUL							9	2	11	2			18	6				
	AUG	31	4	4	1									84	8	2	2		
	SEPT													4	2				
	OCT																		
1912	MAY																		
	JUN							2	2					5	2				
	JUL	7	2											42	7				
	AUG	11	3											62	15				
	SEPT	1	1											5	2				
	OCT																		
1913	MAY																		
	JUN													1	1				
	JUL													12	4				
	AUG													14	5				
	SEPT													29	7				
	OCT													1	1				

Table A2. *Cont.*

Year	Month	TDI [27,29)		TDI [29,32)		TDI ≥ 32		HMDX [38,40)		HMDX [40,45)		HMDX ≥ 45		HI [32,44)		HI [41,54)		HI ≥ 54	
		Total Hours	Days	Total Hours	Days	Total Hours	Days	Total Hours	Days	Total Hours	Days	Total Hours	Days	Total Hours	Days	Total Hours	Days	Total Hours	Days
1914	MAY																		
	JUN													1	1				
	JUL	1	1					6	3					32	10				
	AUG	20	5											68	11				
	SEPT																		
	OCT																		
1915	MAY																		
	JUN													5	2				
	JUL	6	4											80	18				
	AUG													34	7				
	SEPT													7	1				
	OCT																		
1916	MAY																		
	JUN	22	5	1	1			7	1	7	2			112	17	2	1		
	JUL	44	5					26	4	1	1			145	18				
	AUG													26	8				
	SEPT																		
	OCT																		
1917	MAY																		
	JUN																		
	JUL	5	2					2	1					82	14				
	AUG	13	5					4	2					117	21				
	SEPT													10	3				
	OCT																		
1918	MAY																		
	JUN	14	2					5	1					29	5				
	JUL	13	6					1	1					96	17				
	AUG													61	12				
	SEPT	1	1											23	6				
	OCT																		
1919	MAY																		
	JUN													10	2				
	JUL	6	4					2	1					51	10				
	AUG	1	1											21	8				
	SEPT																		
	OCT																		
1920	MAY																		
	JUN													11	2				
	JUL	14	3					5	1	3	1			86	14				
	AUG	51	10					20	5	1	1			133	19				
	SEPT																		
	OCT																		
1921	MAY																		
	JUN																		
	JUL	2	1											118	22				
	AUG	2	1											116	21				
	SEPT													8	2				
	OCT																		
1922	MAY																		
	JUN													10	6				
	JUL	3	2											120	22	1	1		
	AUG	31	8					12	3	4	1			143	18	2	1		
	SEPT													7	4				
	OCT																		

Table A2. *Cont.*

Year	Month	TDI [27,29)		TDI [29,32)		TDI ≥ 32		HMDX [38,40)		HMDX [40,45)		HMDX ≥ 45		HI [32,44)		HI [41,54)		HI ≥ 54	
		Total Hours	Days	Total Hours	Days	Total Hours	Days	Total Hours	Days	Total Hours	Days	Total Hours	Days	Total Hours	Days	Total Hours	Days	Total Hours	Days
1923	MAY													2	2				
	JUN													22	5				
	JUL	15	4					2	1					77	13				
	AUG	4	1											59	11				
	SEPT													24	7				
	OCT																		
1924	MAY																		
	JUN	1	1											27	5				
	JUL	4	2					1	1					121	22				
	AUG	33	7					10	3	3	1			101	16				
	SEPT	8	3					2	1					64	13				
	OCT																		
1925	MAY																		
	JUN													4	1				
	JUL	3	1											99	18				
	AUG	2	2											92	18				
	SEPT	1	1											26	6				
	OCT																		
1926	MAY																		
	JUN	2	1											14	4				
	JUL	4	2	3	1					3	1			47	10				
	AUG	1	1											44	9				
	SEPT													10	3				
	OCT																		
1927	MAY													6	1				
	JUN	11	4	1	1			1	1	1	1			68	16				
	JUL	31	10					4	2	2	1			165	25				
	AUG	25	8	1	1			11	3	1	1			168	23				
	SEPT	4	2					2	1					37	9				
	OCT																		
1928	MAY																		
	JUN	5	3					1	1					65	10				
	JUL	5	3											174	22				
	AUG	7	5											174	26				
	SEPT													26	8				
	OCT													7	2				
1929	MAY													2	1				
	JUN													16	5				
	JUL	10	4											99	16				
	AUG	19	7					3	3					157	25				
	SEPT													6	2				
	OCT																		
1930	MAY													2	1				
	JUN													22	5				
	JUL	5	2											91	18				
	AUG	9	2					4	2					109	15				
	SEPT													16	8				
	OCT																		
1931	MAY																		
	JUN	7	1					3	1	2	1			56	11				
	JUL	21	9					4	1					169	25				
	AUG	31	8					6	3					155	23				
	SEPT	7	4					1	1					35	6				
	OCT																		

Table A2. *Cont.*

Year	Month	TDI [27,29)		TDI [29,32)		TDI ≥ 32		HMDX [38,40)		HMDX [40,45)		HMDX ≥ 45		HI [32,44)		HI [41,54)		HI ≥ 54	
		Total Hours	Days	Total Hours	Days	Total Hours	Days	Total Hours	Days	Total Hours	Days	Total Hours	Days	Total Hours	Days	Total Hours	Days	Total Hours	Days
1932	MAY																		
	JUN													22	7				
	JUL	15	8					5	2					101	17				
	AUG													40	13				
	SEPT	1	1											22	7				
	OCT													9	3				
1933	MAY																		
	JUN													8	3				
	JUL	29	5					7	3					51	8				
	AUG	12	7											82	15				
	SEPT	1	1											4	1				
	OCT																		
1934	MAY																		
	JUN	11	4					3	2					45	10				
	JUL	44	5	3	2			18	2	8	2			120	17	3	1		
	AUG	31	8					6	2	2	1			116	24				
	SEPT													3	1				
	OCT																		
1935	MAY													1	1				
	JUN	18	4					2	2					58	11				
	JUL	14	4	1	1			4	2	1	1			91	14	1	1		
	AUG	25	7					11	2	2	2			90	20				
	SEPT	1	1											23	6				
	OCT													1	1				
1936	MAY																		
	JUN													3	2				
	JUL	54	11					16	6	1	1			160	22				
	AUG	31	5					10	2	2	1			125	21				
	SEPT																		
	OCT																		
1937	MAY																		
	JUN	2	1											19	6				
	JUL	99	16	2	1			43	8	5	3			174	24	1	1		
	AUG	14	4	1	1			2	1	1	1			117	23				
	SEPT	1	1											16	7				
	OCT													1	1				
1938	MAY																		
	JUN	18	6					6	3	1	1			68	8				
	JUL	44	11	1	1			11	4	1	1			191	29				
	AUG	36	12					3	2					150	25				
	SEPT	2	2											21	8				
	OCT																		
1939	MAY																		
	JUN	4	1					2	1					27	4				
	JUL	91	12	4	2			38	5	11	3			170	16	3	2		
	AUG	51	7					23	4	3	2			108	13				
	SEPT	3	2											20	6				
	OCT													8	2				
1940	MAY																		
	JUN	1	1											1	1				
	JUL	44	11					12	4	1	1			151	21				
	AUG	11	4											64	11				
	SEPT																		
	OCT																		

Table A2. *Cont.*

Year	Month	TDI [27,29)		TDI [29,32)		TDI ≥ 32		HMDX [38,40)		HMDX [40,45)		HMDX ≥ 45		HI [32,44)		HI [41,54)		HI ≥ 54	
		Total Hours	Days	Total Hours	Days	Total Hours	Days	Total Hours	Days	Total Hours	Days	Total Hours	Days	Total Hours	Days	Total Hours	Days	Total Hours	Days
1941	MAY													4	1				
	JUN													2	2				
	JUL	64	11					23	6	2	1			153	23				
	AUG	44	8	2	2			22	2	3	2			130	22				
	SEPT																		
	OCT																		
1942	MAY													4	1				
	JUN	24	4					4	1	6	1			66	9	2	1		
	JUL	19	5					6	1	2	2			83	16				
	AUG	8	4											70	14				
	SEPT													12	5				
	OCT																		
1943	MAY																		
	JUN	2	1											17	4				
	JUL	23	7	1	1			6	1	2	1			84	14				
	AUG	35	10					7	3					131	23				
	SEPT	7	4											41	8				
	OCT													12	3				
1944	MAY													4	1				
	JUN	1	1											22	6				
	JUL	23	6					6	4					80	16				
	AUG	6	3					1	1					83	18				
	SEPT	3	2											41	9				
	OCT																		
1945	MAY													18	5				
	JUN	11	2					5	1					28	7				
	JUL	24	4	6	1			9	3	6	1			121	18	1	1		
	AUG	130	13	14	6			59	10	23	6			201	19	2	1		
	SEPT													25	5				
	OCT																		
1946	MAY																		
	JUN													32	10				
	JUL	41	7					17	5	2	1			140	20				
	AUG	40	8	1	1			8	2	1	1			199	26	1	1		
	SEPT	5	2					2	1					66	10				
	OCT																		
1947	MAY																		
	JUN													13	3				
	JUL	29	7					4	2					110	16				
	AUG	42	10					6	4	1	1			127	22				
	SEPT																		
	OCT																		
1948	MAY																		
	JUN	2	1											16	4				
	JUL	5	1											48	9				
	AUG	21	8					4	3					118	20				
	SEPT													6	1				
	OCT																		
1949	MAY																		
	JUN													6	2				
	JUL	13	2					2	2					75	13				
	AUG	4	1											41	7				
	SEPT													2	1				
	OCT																		

Table A2. *Cont.*

Year	Month	TDI [27,29)		TDI [29,32)		TDI ≥ 32		HMDX [38,40)		HMDX [40,45)		HMDX ≥ 45		HI [32,44)		HI [41,54)		HI ≥ 54	
		Total Hours	Days	Total Hours	Days	Total Hours	Days	Total Hours	Days	Total Hours	Days	Total Hours	Days	Total Hours	Days	Total Hours	Days	Total Hours	Days
1950	MAY													14	2				
	JUN	12	3					5	1					52	9				
	JUL	9	4					2	1					149	22				
	AUG	13	4					2	1					100	17				
	SEPT													22	7				
	OCT																		
1951	MAY																		
	JUN	1	1											18	5				
	JUL	18	5					6	3					90	16				
	AUG	68	8	6	2			24	5	10	3			148	18	2	1		
	SEPT	2	1											17	5				
	OCT																		
1952	MAY													2	2				
	JUN	8	2											39	7				
	JUL	12	4											56	13				
	AUG	91	16	7	2			32	7	20	5			224	27	5	2		
	SEPT	27	8					3	2					100	18				
	OCT																		
1953	MAY																		
	JUN													9	5				
	JUL	9	2					1	1					98	20				
	AUG	3	2											53	10				
	SEPT													3	3				
	OCT																		
1954	MAY																		
	JUN	2	1											54	11				
	JUL	51	11					16	4	1	1			144	23				
	AUG	26	8					8	2					119	23				
	SEPT	2	1											15	6				
	OCT																		
1955	MAY													4	2				
	JUN	1	1											32	7				
	JUL	15	6					3	2					79	17				
	AUG													23	6				
	SEPT																		
	OCT																		
1956	MAY																		
	JUN	4	1					2	1					38	7				
	JUL	46	7	4	1			21	2	7	3			115	16				
	AUG	60	13	1	1			20	6	1	1			174	28				
	SEPT	18	3					10	2					41	8				
	OCT																		
1957	MAY																		
	JUN	17	5					2	1	1	1			55	9				
	JUL	12	4											89	21				
	AUG	62	9					19	5	1	1			134	17				
	SEPT													1	1				
	OCT																		
1958	MAY																		
	JUN	6	2							1	1			22	4				
	JUL	9	4											101	18				
	AUG	46	7	1	1			22	3	9	3			133	18				
	SEPT																		
	OCT																		

Table A2. *Cont.*

Year	Month	TDI [27,29)		TDI [29,32)		TDI ≥ 32		HMDX [38,40)		HMDX [40,45)		HMDX ≥ 45		HI [32,44)		HI [41,54)		HI ≥ 54	
		Total Hours	Days	Total Hours	Days	Total Hours	Days	Total Hours	Days	Total Hours	Days	Total Hours	Days	Total Hours	Days	Total Hours	Days	Total Hours	Days
1959	MAY													3	1				
	JUN																		
	JUL	5	1											86	17				
	AUG													49	11				
	SEPT																		
	OCT																		
1960	MAY													1	1				
	JUN													20	5				
	JUL	3	3					1	1					86	17				
	AUG	10	4					2	2					89	16				
	SEPT													15	6				
	OCT																		
1961	MAY													1	1				
	JUN	3	1											19	4				
	JUL	11	4					4	4					60	11				
	AUG	7	4											81	13				
	SEPT													17	3				
	OCT																		
1962	MAY																		
	JUN													32	9				
	JUL	19	7					1	1					112	16				
	AUG	21	6					4	3					179	23				
	SEPT													26	6				
	OCT																		
1963	MAY																		
	JUN	11	4											57	9				
	JUL	15	3					1	1					102	16				
	AUG	50	7	4	2			17	3	7	2			152	22	2	1		
	SEPT	4	2					1	1					28	5				
	OCT																		
1964	MAY																		
	JUN	1	1											7	3				
	JUL	2	1											39	10				
	AUG	3	1											25	6				
	SEPT													1	1				
	OCT																		
1965	MAY																		
	JUN													21	7				
	JUL	33	10					13	2					127	16				
	AUG	1	1											37	7				
	SEPT													9	4				
	OCT																		
1966	MAY																		
	JUN													10	2				
	JUL	11	6					2	2					105	19				
	AUG	31	11					8	6					151	22				
	SEPT																		
	OCT																		
1967	MAY																		
	JUN													4	1				
	JUL	2	1											33	7				
	AUG	38	9					12	3	1	1			106	18				
	SEPT																		
	OCT																		

Table A2. *Cont.*

Year	Month	TDI [27,29)		TDI [29,32)		TDI ≥ 32		HMDX [38,40)		HMDX [40,45)		HMDX ≥ 45		HI [32,44)		HI [41,54)		HI ≥ 54	
		Total Hours	Days	Total Hours	Days	Total Hours	Days	Total Hours	Days	Total Hours	Days	Total Hours	Days	Total Hours	Days	Total Hours	Days	Total Hours	Days
1968	MAY													3	2				
	JUN	2	1					1	1					30	4				
	JUL	21	5					6	3					104	12				
	AUG	1	1											28	5				
	SEPT	1	1											3	2				
	OCT																		
1969	MAY	3	1					1	1					11	2				
	JUN	2	1											26	4				
	JUL													7	3				
	AUG	11	3											48	11				
	SEPT	1	1					1	1					9	4				
	OCT																		
1970	MAY																		
	JUN													10	5				
	JUL	1	1											60	15				
	AUG	9	3					3	1					81	17				
	SEPT													3	2				
	OCT																		
1971	MAY																		
	JUN	3	1					1	1					31	7				
	JUL	1	1											37	8				
	AUG	10	4											87	18				
	SEPT																		
	OCT																		
1972	MAY																		
	JUN													24	3				
	JUL	6	4											52	11				
	AUG	10	4											83	13				
	SEPT	2	1											3	1				
	OCT																		
1973	MAY													2	1				
	JUN													9	3				
	JUL	65	9	8	2			21	3	18	4			136	17				
	AUG													4	1				
	SEPT													7	2				
	OCT																		
1974	MAY																		
	JUN	2	2					1	1					20	6				
	JUL	13	3											93	14				
	AUG	3	2											50	13				
	SEPT													1	1				
	OCT																		
1975	MAY																		
	JUN													19	7				
	JUL	15	5					3	2					91	16				
	AUG	1	1											19	7				
	SEPT	1	1											16	6				
	OCT																		
1976	MAY																		
	JUN																		
	JUL	8	4											28	10				
	AUG	11	4							1	1			30	8				
	SEPT													1	1				
	OCT																		

Table A2. *Cont.*

Year	Month	TDI [27,29)		TDI [29,32)		TDI ≥ 32		HMDX [38,40)		HMDX [40,45)		HMDX ≥ 45		HI [32,44)		HI [41,54)		HI ≥ 54	
		Total Hours	Days	Total Hours	Days	Total Hours	Days	Total Hours	Days	Total Hours	Days	Total Hours	Days	Total Hours	Days	Total Hours	Days	Total Hours	Days
1977	MAY																		
	JUN													28	8				
	JUL	38	9					14	3	1	1			130	20				
	AUG	15	6					1	1					107	19				
	SEPT													1	1				
	OCT																		
1978	MAY																		
	JUN	11	3					1	1					57	9				
	JUL	46	11					9	5					124	17				
	AUG	5	1					1	1					34	6				
	SEPT																		
	OCT																		
1979	MAY																		
	JUN	6	3											40	6				
	JUL	32	7					7	3	1	1			80	13				
	AUG	16	3	1	1			1	1	1	1			63	12				
	SEPT	1	1											12	3				
	OCT																		
1980	MAY																		
	JUN													31	7				
	JUL	31	8	8	1			5	2	9	1			134	20	5	1		
	AUG	35	4	1	1			16	3	2	1			74	16				
	SEPT													1	1				
	OCT																		
1981	MAY																		
	JUN	24	3					10	2					57	7				
	JUL	7	2					1	1					47	10				
	AUG	2	1											47	13				
	SEPT													2	2				
	OCT																		
1982	MAY													3	1				
	JUN	38	5	5	1			14	2	8	1	1	1	71	8			1	1
	JUL	7	3					1	1					62	14				
	AUG	18	9					3	2					88	17				
	SEPT	10	3					3	1					21	3				
	OCT																		
1983	MAY																		
	JUN	5	1											7	2				
	JUL	25	6					4	3					80	17				
	AUG	8	3											40	9				
	SEPT													4	2				
	OCT																		
1984	MAY																		
	JUN													9	2				
	JUL	30	7					5	1					90	15				
	AUG	1	1											28	7				
	SEPT													5	2				
	OCT	1	1											6	4				
1985	MAY																		
	JUN	3	1											31	7				
	JUL	16	3					5	3					85	14				
	AUG	17	5	4	1			9	1	5	1			96	19				
	SEPT													12	3				
	OCT																		

Table A2. *Cont.*

Year	Month	TDI [27,29)		TDI [29,32)		TDI ≥ 32		HMDX [38,40)		HMDX [40,45)		HMDX ≥ 45		HI [32,44)		HI [41,54)		HI ≥ 54	
		Total Hours	Days	Total Hours	Days	Total Hours	Days	Total Hours	Days	Total Hours	Days	Total Hours	Days	Total Hours	Days	Total Hours	Days	Total Hours	Days
1986	MAY																		
	JUN	1	1											11	4				
	JUL	35	9					2	1					92	19				
	AUG	36	8	2	2			10	2	2	2			146	29				
	SEPT	1	1											27	7				
	OCT																		
1987	MAY																		
	JUN	27	6					4	2					75	12				
	JUL	86	6	53	8			33	4	65	5	3	3	186	15	33	7		
	AUG	68	12	5	4			22	5	7	4			131	19	1	1		
	SEPT	12	5											56	11				
	OCT																		
1988	MAY																		
	JUN	1	1											26	9				
	JUL	92	14	20	3			36	7	24	4			204	24	9	2		
	AUG	36	10					6	3					148	27				
	SEPT	15	4					2	2					32	6				
	OCT																		
1989	MAY																		
	JUN													3	2				
	JUL	8	4					3	2					69	15				
	AUG	2	1											108	23				
	SEPT													7	3				
	OCT																		
1990	MAY													8	2				
	JUN	13	3					4	1	1	1			41	8				
	JUL	76	11	9	4			26	3	14	7			178	23	3	2		
	AUG	6	3											79	16				
	SEPT	2	1					1	1					27	7				
	OCT																		
1991	MAY																		
	JUN	1	1											55	11				
	JUL	18	4											88	15				
	AUG	32	8					11	4					78	15				
	SEPT													2	1				
	OCT	2												12	2				
1992	MAY																		
	JUN	1	1											15	5				
	JUL	15	4					1	1					39	7				
	AUG	31	10	3	1			10	2	3	1			162	27	1	1		
	SEPT	2	2											16	4				
	OCT																		
1993	MAY													4	1				
	JUN	8	3					1	1					48	8				
	JUL	71	14					19	5					168	23				
	AUG	40	5	3	2			18	3	7	3			145	24	1	1		
	SEPT	3	1											22	5				
	OCT													1	1				
1994	MAY	10	4					1	1					40	6				
	JUN	9	3					2	2					50	8				
	JUL	41	10	1	1			8	3	1	1			117	17				
	AUG	98	13	8	4			45	4	19	7			212	26	2	2		
	SEPT	4	2											95	19				
	OCT													3	1				

Table A2. *Cont.*

Year	Month	TDI [27,29)		TDI [29,32)		TDI ≥ 32		HMDX [38,40)		HMDX [40,45)		HMDX ≥ 45		HI [32,44)		HI [41,54)		HI ≥ 54	
		Total Hours	Days	Total Hours	Days	Total Hours	Days	Total Hours	Days	Total Hours	Days	Total Hours	Days	Total Hours	Days	Total Hours	Days	Total Hours	Days
1995	MAY																		
	JUN	22	7	3	1	5	2	6	3	6	1	5	2	71	15	3	1	5	2
	JUL	33	10					8	4					142	23				
	AUG	17	6					2	1					79	18				
	SEPT	2	1											7	3				
	OCT																		
1996	MAY																		
	JUN	5	4											52	10				
	JUL	12	5					1	1					58	10				
	AUG	35	10					3	2					120	22				
	SEPT													3	1				
	OCT																		
1997	MAY													2	2				
	JUN	29	9					7	2					90	13				
	JUL	29	10					9	3	1	1			128	24				
	AUG	24	8											67	13				
	SEPT													3	2				
	OCT																		
1998	MAY																		
	JUN	18	3					9	2					57	12				
	JUL	62	11	20	3	1	1	17	3	20	4	5	1	195	23	14	3		
	AUG	86	20					27	10					208	28				
	SEPT																		
	OCT																		
1999	MAY																		
	JUN	4	4											85	17				
	JUL	98	20					43	10	2	2			205	28				
	AUG	118	11	24	6			56	4	44	9			215	18	11	5		
	SEPT													6	4				
	OCT													1	1				
2000	MAY													1	1				
	JUN	20	5					6	3					103	17				
	JUL	93	10	33	6			36	4	38	6	1	1	207	18	21	6		
	AUG	18	6					6		1	1			148	23				
	SEPT	9	4					2	1					43	8				
	OCT																		
2001	MAY													3	3				
	JUN	7	1					3	1					50	13				
	JUL	141	14	34	11			61	7	50	13			266	25	7	5		
	AUG	64	7	12	4			31	1	22	7			190	26	1	1		
	SEPT	2	2											29	8				
	OCT																		
2002	MAY																		
	JUN	15	3					4	2					60	11				
	JUL	70	16					14	7					202	27				
	AUG	20	5					7	2					80	17				
	SEPT													1	1				
	OCT																		
2003	MAY													7	2				
	JUN	10	6											122	20				
	JUL	58	12					20	4	2	1			189	30				
	AUG	72	15	1	1			14	4	2	1			212	28				
	SEPT	15	3					7	1					26	3				
	OCT																		

Table A2. *Cont.*

Year	Month	TDI [27,29)		TDI [29,32)		TDI ≥ 32		HMDX [38,40)		HMDX [40,45)		HMDX ≥ 45		HI [32,44)		HI [41,54)		HI ≥ 54	
		Total Hours	Days	Total Hours	Days	Total Hours	Days	Total Hours	Days	Total Hours	Days	Total Hours	Days	Total Hours	Days	Total Hours	Days	Total Hours	Days
2004	MAY																		
	JUN	48	13	7	1			20	5	9	3			111	18	1	1		
	JUL	130	16	46	7	8	3	59	9	52	9	15	3	216	20	33	6	3	1
	AUG	148	19	18	9			87	12	29	12	1	1	215	26	7	4		
	SEPT	20	4	1	1			11	3	1	1			32	7				
	OCT																		
2005	MAY																		
	JUN	2	2											32	9				
	JUL	174	13	37	12			85	4	58	17	1	1	254	19	17	8		
	AUG	113	17	33	7			45	7	42	8	4	2	212	26	22	5		
	SEPT	11	4					4	3					36	9				
	OCT																		
2006	MAY	27	4	2	1			13	2	4	2			54	8				
	JUN	104	6	36	10			40	2	52	9	1	1	157	11	18	6		
	JUL	107	10	24	7			46	6	38	9			157	15	14	5		
	AUG	165	8	116	22	1	1	73	3	129	20	14	5	271	17	78	14		
	SEPT	19	4					5	1	5	1			34	6				
	OCT													1	1				
2007	MAY													7	2				
	JUN	87	9	16	3			36	6	25	4			149	12	13	3		
	JUL	112	11	25	7			46	6	36	7			253	24	13	3		
	AUG	65	16					25	5					224	28				
	SEPT	12	2					6	1					23	6				
	OCT																		
2008	MAY	5	1					3	1					10	2				
	JUN	23	5					2	2					115	14				
	JUL	69	14					22	7	2	1			197	26				
	AUG	101	17	2	2			32	7	6	4			218	28				
	SEPT	18	7					1	1					64	13				
	OCT																		
2009	MAY													4	2				
	JUN	9	3					2	1					64	10				
	JUL	79	12	2	1			34	6	10	4			209	29				
	AUG	28	8					4	2					127	25				
	SEPT	10	3											25	5				
	OCT																		
2010	MAY													6	3				
	JUN	29	6					10	4					69	9				
	JUL	91	18					36	7	2	2			207	27				
	AUG	172	20	11	6			80	9	28	10			308	29				
	SEPT													11	5				
	OCT																		
2011	MAY																		
	JUN	2	1					1	1					29	6				
	JUL	60	10					14	4	1	1			205	26				
	AUG	32	7	1	1			11	2	1	1			159	26				
	SEPT	5	3											95	18				
	OCT																		
2012	MAY																		
	JUN	20	6					5	2					145	21				
	JUL	180	17	14	8			86	10	34	11			303	26	4	3		
	AUG	115	15	4	3			49	8	16	6			236	27				
	SEPT													48	13				
	OCT													5	1				

Table A2. *Cont.*

Year	Month	TDI [27,29)		TDI [29,32)		TDI ≥ 32		HMDX [38,40)		HMDX [40,45)		HMDX ≥ 45		HI [32,44)		HI [41,54)		HI ≥ 54	
		Total Hours	Days	Total Hours	Days	Total Hours	Days	Total Hours	Days	Total Hours	Days	Total Hours	Days	Total Hours	Days	Total Hours	Days	Total Hours	Days
2013	MAY																		
	JUN	5	3					1	1					71	12				
	JUL	22	5					9	2					135	21				
	AUG	9	4					1	1					140	27				
	SEPT	2	1											11	3				
	OCT																		
2014	MAY																		
	JUN	19	2	1	1			6	1	3	1			46	11				
	JUL	44	13					6	5					133	21				
	AUG	98	19					17	7	1	1			193	27				
	SEPT													6	2				
	OCT																		
2015	MAY																		
	JUN													22	5				
	JUL	70	10	1	1			33	5	5	2			233	27				
	AUG	67	17					22	7					191	26				
	SEPT	31	6					8	4					75	14				
	OCT																		
2016	MAY													2	1				
	JUN	53	9	1	1			21	4	3	2	1	1	125	16	1	1		
	JUL	43	13					4	3					214	29				
	AUG	56	15					10	6					174	23				
	SEPT													6	3				
	OCT																		
2017	MAY													4	2				
	JUN	49	6	5	1			25	4	7	2			94	11	2	1		
	JUL	85	9	14	4			36	4	23	5			203	22	7	2		
	AUG	62	11	1	1			14	3	3	1			182	24				
	SEPT	17	8					1	1					76	17				
	OCT																		
2018	MAY																		
	JUN													22	7				
	JUL	55	16					7	4					184	28				
	AUG	14	5					4	2					166	29				
	SEPT	4	2											42	7				
	OCT																		
2019	MAY																		
	JUN	14	5											106	16				
	JUL	72	13					24	7	1	1			190	23				
	AUG	111	16	7	4			40	10	14	4			213	25	1	1		
	SEPT	3		1	1			2		1	1			26	8				
	OCT																		
2020	MAY													22	5				
	JUN	4	1					1	1					28	6				
	JUL	54	9					18	3	2	2			184	27				
	AUG	27	8	1	1			6	1	2	1			171	26				
	SEPT	7	2											53	13				
	OCT													2	2				
2021	MAY													5	2				
	JUN	66	6	5	2			30	4	10	4			97	8	2	1		
	JUL	118	16	10	3			47	8	15	3			270	29	4	2		
	AUG	142	19	26	6			44	8	36	5	2	1	285	27	15	4		
	SEPT	6	2					2	2					32	7				
	OCT																		

Table A2. *Cont.*

Year	Month	TDI [27,29)		TDI [29,32)		TDI ≥ 32		HMDX [38,40)		HMDX [40,45)		HMDX ≥ 45		HI [32,44)		HI [41,54)		HI ≥ 54	
		Total Hours	Days	Total Hours	Days	Total Hours	Days	Total Hours	Days	Total Hours	Days	Total Hours	Days	Total Hours	Days	Total Hours	Days	Total Hours	Days
2022	MAY													4	3				
	JUN	25	8					1	1					106	19				
	JUL	87	16					21	6	3	3			202	23				
	AUG	52	10					13	5					155	26				
	SEPT	6	4											36	8				
	OCT																		
2023	MAY																		
	JUN	3	2											55	9				
	JUL	187	15	44	9			68	8	65	12	2	1	340	23	21	7		
	AUG	118	20					41	10	2	2			231	28				
	SEPT	2	1											30	7				
	OCT																		
2024	MAY																		
	JUN	81	19					16	5	3	1			226	27				
	JUL	168	24	7	3			67	10	17	7			352	30				
	AUG	140	23					48	11	5	3			274	30				
	SEPT	12	4					3	2					41	10				
	OCT																		

Appendix D

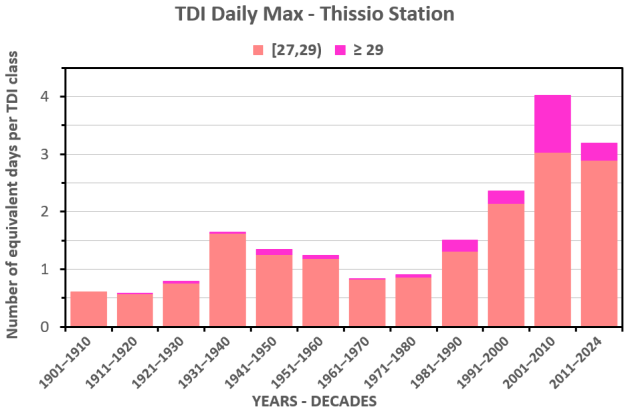

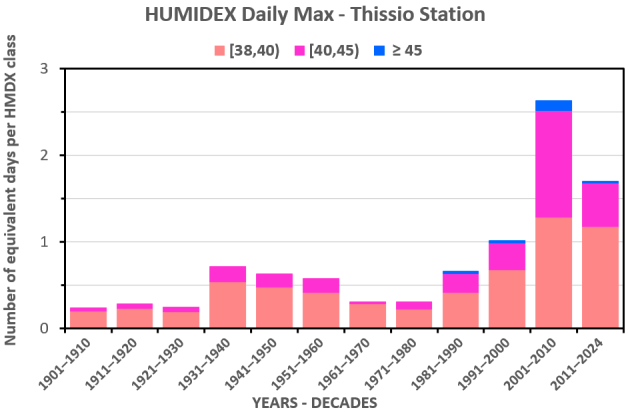

Figure A1. *Cont.*

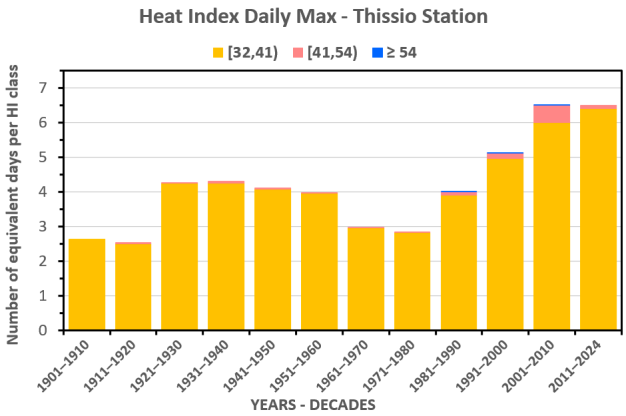

Figure A1. Decadal distribution of thermal discomfort conditions in Athens during the 1901–2024 period, based on the daily maximum values of the TDI (**up**), HMDX (**middle**), and HI (**down**). Each bar represents the total number of days per decade that fall within specific discomfort classes, expressed as equivalent day available in each decade.

References

1. Andersen, H.E.; Larsen, S.E.; Hoffman, C.C.; Jensen, T.S.; Rasmussen, E.K. Climate-Change Impacts on Hydrology and Nutrients in a Danish Lowland River Basin. *Sci. Total Environ.* **2006**, *365*, 223–237. [CrossRef]
2. Da, Y.; Xu, Y.; McCarl, B. Effects of Surface Ozone and Climate on Historical (1980–2015) Crop Yields in the United States: Implication for Mid-21st Century Projection. *Environ. Resour. Econ.* **2022**, *81*, 355–378. [CrossRef]
3. Jing, X.; Jiang, S.; Liu, H.; Li, Y.; He, J.S. Complex Relationships and Feedback Mechanisms between Climate Change and Biodiversity. *Biodivers. Sci.* **2022**, *30*, 22462. [CrossRef]
4. Shen, F.; Yang, L.; Zhang, L.; Guo, M.; Huang, H.; Zhou, C. Quantifying the Direct Effects of Long-Term Dynamic Land Use Intensity on Vegetation Change and Its Interacted Effects with Economic Development and Climate Change in Jiangsu, China. *J. Environ. Manag.* **2023**, *325*, 116562. [CrossRef] [PubMed]
5. Alimonti, G.; Mariani, L.; Prodi, F.; Ricci, R.A. A Critical Assessment of Extreme Events Trends in Times of Global Warming. *Eur. Phys. J. Plus* **2022**, *137*, 112. [CrossRef]
6. Clarke, B.; Otto, F.; Stuart-Smith, R.; Harrington, L. Extreme Weather Impacts of Climate Change: An Attribution Perspective. *Environ. Res. Clim.* **2022**, *1*, 012001. [CrossRef]
7. Amirkhani, M.; Ghaemimood, S.; von Schreeb, J.; El-Khatib, Z.; Yaya, S. Extreme Weather Events and Death Based on Temperature and CO_2 Emission—A Global Retrospective Study in 77 Low-, Middle- and High-Income Countries from 1999 to 2018. *Prev. Med. Rep.* **2022**, *28*, 101846. [CrossRef]
8. Laino, E.; Iglesias, G. Extreme Climate Change Hazards and Impacts on European Coastal Cities: A Review. *Renew. Sustain. Energy Rev.* **2023**, *184*, 113587. [CrossRef]
9. Laino, E.; Iglesias, G. Scientometric Review of Climate-Change Extreme Impacts on Coastal Cities. *Ocean Coast. Manag.* **2023**, *242*, 106709. [CrossRef]
10. Pachauri, R.K.; Reisinger, A. *Climate Change 2007: Synthesis Report. Contribution of Working Groups I, II and III to the Fourth Assessment Report of the Intergovernmental Panel on Climate Change*; IPCC: Geneva, Switzerland, 2007.
11. IPCC. *Climate Change 2014: Synthesis Report. Contribution of Working Groups I, II and III to the Fifth Assessment Report of the Intergovernmental Panel on Climate Change*; IPCC: Geneva, Switzerland, 2014.
12. Skendžić, S.; Zovko, M.; Živković, I.P.; Lešić, V.; Lemić, D. The Impact of Climate Change on Agricultural Insect Pests. *Insects* **2021**, *12*, 440. [CrossRef]
13. Nastos, P.T.; Matzarakis, A. Weather Impacts on Respiratory Infections in Athens, Greece. *Int. J. Biometeorol.* **2006**, *50*, 358–369. [CrossRef]
14. He, B.J.; Wang, J.; Liu, H.; Ulpiani, G. Localized Synergies between Heat Waves and Urban Heat Islands: Implications on Human Thermal Comfort and Urban Heat Management. *Environ. Res.* **2021**, *193*, 110584. [CrossRef]
15. Ren, Z.; Fu, Y.; Dong, Y.; Zhang, P.; He, X. Rapid Urbanization and Climate Change Significantly Contribute to Worsening Urban Human Thermal Comfort: A National 183-City, 26-Year Study in China. *Urban Clim.* **2022**, *43*, 101154. [CrossRef]
16. Isinkaralar, K.; Isinkaralar, O.; Bayraktar, E.P. Ecological and Health Risk Assessment in Road Dust Samples from Various Land Use of Düzce City Center: Towards the Sustainable Urban Development. *Water Air Soil Pollut.* **2024**, *235*, 84. [CrossRef]
17. Lin, Z.; Deng, S. A Study on the Thermal Comfort in Sleeping Environments in the Subtropics—Developing a Thermal Comfort Model for Sleeping Environments. *Build. Environ.* **2008**, *43*, 70–81. [CrossRef]

18. Kurmi, R.S.; Gupta, J.K. *A Textbook of Refrigeration and Air Conditioning*, 1st ed.; Eurasia Publishing House: New Delhi, India, 2006.
19. Isinkaralar, O.; Isinkaralar, K. Projection of Bioclimatic Patterns via CMIP6 in the Southeast Region of Türkiye: A Guidance for Adaptation Strategies for Climate Policy. *Environ. Monit. Assess.* **2023**, *195*, 1448. [CrossRef]
20. de Freitas, C.R.; Grigorieva, E.A. A Comparison and Appraisal of a Comprehensive Range of Human Thermal Climate Indices. *Int. J. Biometeorol.* **2015**, *61*, 487–512. [CrossRef]
21. McLaughlin, S.; Cooper, J.A.G. A Multi-Scale Coastal Vulnerability Index: A Tool for Coastal Managers? *Environ. Hazards* **2010**, *9*, 233–248. [CrossRef]
22. Rabby, Y.W.; Hossain, M.B.; Hasan, M.U. Social Vulnerability in the Coastal Region of Bangladesh: An Investigation of Social Vulnerability Index and Scalar Change Effects. *Int. J. Disaster Risk Reduct.* **2019**, *41*, 101329. [CrossRef]
23. Tasnuva, A.; Hossain, M.R.; Salam, R.; Islam, A.R.M.T.; Patwary, M.M.; Ibrahim, S.M. Employing Social Vulnerability Index to Assess Household Social Vulnerability of Natural Hazards: An Evidence from Southwest Coastal Bangladesh. *Environ. Dev. Sustain.* **2021**, *23*, 10223–10245. [CrossRef]
24. Pantusa, D.; D'Alessandro, F.; Frega, F.; Francone, A.; Tomasicchio, G.R. Improvement of a Coastal Vulnerability Index and Its Application along the Calabria Coastline, Italy. *Sci. Rep.* **2022**, *12*, 21959. [CrossRef]
25. Kovaleva, O.; Sergeev, A.; Ryabchuk, D. Coastal Vulnerability Index as a Tool for Current State Assessment and Anthropogenic Activity Planning for the Eastern Gulf of Finland Coastal Zone (the Baltic Sea). *Appl. Geogr.* **2022**, *143*, 102710. [CrossRef]
26. Oloyede, M.O.; Williams, A.B.; Ode, G.O.; Benson, N.U. Coastal Vulnerability Assessment: A Case Study of the Nigerian Coastline. *Sustainability* **2022**, *14*, 2097. [CrossRef]
27. Šimac, Z.; Lončar, N.; Faivre, S. Overview of Coastal Vulnerability Indices with Reference to Physical Characteristics of the Croatian Coast of Istria. *Hydrology* **2023**, *10*, 14. [CrossRef]
28. Esmaeili, R.; Gandomkar, A.; Nokhndan, M.H. Assessment of Comfortable Climate in Several Main Iranian Tourism Cities Using Physiologic Equivalence Temperature Index. *Phys. Geogr. Res. Q.* **2011**, *75*, 8–10. [CrossRef]
29. Thom, E.C. The Discomfort Index. *Weatherwise* **1959**, *12*, 57–61. [CrossRef]
30. Masterton, J.M.; Richardson, F.A. *Humidex: A Method of Quantifying Human Discomfort Due to Excessive Heat and Humidity*; Technical Report No. 45; Atmospheric Environment Service, Environment Canada: Downsview, ON, Canada, 1979.
31. Steadman, R.G. The Assessment of Sultriness. Part I: A Temperature–Humidity Index Based on Human Physiology and Clothing Science. *J. Appl. Meteorol.* **1979**, *18*, 861–873. [CrossRef]
32. Steadman, R.G. The Assessment of Sultriness. Part II: Effects of Wind, Extra Radiation and Barometric Pressure on Apparent Temperature. *J. Appl. Meteorol.* **1979**, *18*, 874–885. [CrossRef]
33. Rothfusz, L.P. *The Heat Index "Equation"*; Technical Attachment SR/SSD 90-23; National Weather Service, Southern Region Headquarters: Fort Worth, TX, USA, 1990.
34. Yousif, T.A.; Tahir, H.M. The Relationship between Relative Humidity and the Dew Point Temperature in Khartoum State, Sudan. *J. Appl. Ind. Sci.* **2013**, *1*, 20–23.
35. Epstein, Y.; Moran, D.S. Thermal Comfort and the Heat Stress Indices. *Ind. Health* **2006**, *44*, 388–398. [CrossRef]
36. Stathopoulou, M.I.; Cartalis, C.; Keramitsoglou, I.; Santamouris, M. Thermal Remote Sensing of Thom's Discomfort Index (DI): Comparison with In-Situ Measurements. *Remote Sens.* **2005**, *5983*, 131–139. [CrossRef]
37. Adegoke, O.O.; Dombo, T.P. Geospatial Modeling of Human Thermal Comfort in Akure Metropolis Using Thom's Discomfort Index. *Int. J. Environ. Bioenergy* **2019**, *14*, 40–55. [CrossRef]
38. Talukdar, M.S.J.; Hossen, M.S.; Baten, M.A. Trends of Outdoor Thermal Discomfort in Mymensingh: An Application of Thom's Discomfort Index. *J. Environ. Sci. Nat. Resour.* **2017**, *10*, 151–156. [CrossRef]
39. Ehsan, S.; Abbas, F.; Ibrahim, M.; Ahmad, B.; Farooque, A.A. Thermal Discomfort Levels, Building Design Concepts, and Some Heat Mitigation Strategies in Low-Income Communities of a South Asian City. *Int. J. Environ. Res. Public Health* **2021**, *18*, 2535. [CrossRef]
40. Monforte, P.; Ragusa, M.A. Evaluation of Bioclimatic Discomfort Trend in a Central Area of the Mediterranean Sea. *Climate* **2022**, *10*, 146. [CrossRef]
41. Maftei, C.; Buta, C. Application of Thermal Discomfort Indices for the Coastal Zone of Black Sea, in Dobrogea Region. *Ovidius Univ. Ann. Ser. Civ. Eng.* **2017**, *19*, 87–100. [CrossRef]
42. Azevedo, P.V.; Bezerra, P.T.C.; Leitão, M.M.V.B.R.; Santos, C.A.C. Thermal Comfort Level Assessment in Urban Area of Petrolina-PE County, Brazil. *Rev. Bras. Meteorol.* **2017**, *32*, 555–563. [CrossRef]
43. Diaconescu, E.; Sankare, H.; Chow, K.; Murdock, T.Q.; Cannon, A.J. A Short Note on the Use of Daily Climate Data to Calculate Humidex Heat-Stress Indices. *Int. J. Climatol.* **2023**, *43*, 837–849. [CrossRef]
44. Orimoloye, I.R.; Mazinyo, S.P.; Nel, W.; Iortyom, E.T. Climate Variability and Heat Stress Index Have Increasing Potential Ill-Health and Environmental Impacts in East London, South Africa. *Int. J. Appl. Eng. Res.* **2017**, *12*, 6910–6918.
45. Golbabaei, F.; Heidari, H.; Shamsipour, A. The Assessment of Thermal Conditions Using Humidex in Different Weather Conditions: A Case in Different Climates of Iran. *J. Health Sci. Surveill. Syst.* **2021**, *9*, 127–134. [CrossRef]

46. FallahGhalhari, G.; FarhangDehghan, S.; Asghari, M. Trend Analysis of Humidex as a Heat Discomfort Index Using Mann–Kendall and Sen's Slope Estimator Statistical Tests. *Environ. Health Eng. Manag. J.* **2022**, *9*, 165–176. [CrossRef]
47. Scoccimarro, E.; Fogli, P.G.; Gualdi, S. The Role of Humidity in Determining Scenarios of Perceived Temperature Extremes in Europe. *Environ. Res. Lett.* **2017**, *12*, 114029. [CrossRef]
48. Středová, H.; Středa, T.; Litschmann, T. Smart Tools of Urban Climate Evaluation for Smart Spatial Planning. *Morav. Geogr. Rep.* **2015**, *23*, 47–57. [CrossRef]
49. Infusino, E.; Caloiero, T.; Fusto, F.; Calderaro, G.; Brutto, A.; Tagarelli, G. Characterization of the 2017 Summer Heat Waves and Their Effects on the Population of an Area of Southern Italy. *Int. J. Environ. Res. Public Health* **2021**, *18*, 970. [CrossRef]
50. Dahl, K.; Licker, R.; Abatzoglou, J.T.; Declet-Barreto, J. Increased Frequency of and Population Exposure to Extreme Heat Index Days in the United States during the 21st Century. *Environ. Res. Commun.* **2019**, *1*, 075002. [CrossRef]
51. Michelozzi, P.; Accetta, G.; De Sario, M.; D'Ippoliti, D.; Marino, C.; Baccini, M.; Biggeri, A.; Anderson, H.R.; Katsouyanni, K.; Ballester, F.; et al. High Temperature and Hospitalizations for Cardiovascular and Respiratory Causes in 12 European Cities. *Am. J. Respir. Crit. Care Med.* **2009**, *179*, 383–389. [CrossRef] [PubMed]
52. Khalaj, B.; Lloyd, G.; Sheppeard, V.; Dear, K. The Health Impacts of Heat Waves in Five Regions of New South Wales, Australia: A Case-Only Analysis. *Int. Arch. Occup. Environ. Health* **2010**, *83*, 833–842. [CrossRef]
53. Kyselý, J.; Kim, J. Mortality during Heat Waves in South Korea, 1991 to 2005: How Exceptional Was the 1994 Heat Wave? *Clim. Res.* **2009**, *38*, 105–116. [CrossRef]
54. Bell, M.L.; O'Neill, M.S.; Ranjit, N.; Borja-Aburto, V.H.; Cifuentes, L.A.; Gouveia, N.C. Vulnerability to Heat-Related Mortality in Latin America: A Case-Crossover Study in São Paulo, Brazil, Santiago, Chile and Mexico City, Mexico. *Int. J. Epidemiol.* **2008**, *37*, 796–804. [CrossRef]
55. Angouridakis, V.E.; Makrogiannis, T.J. The Discomfort-Index in Thessaloniki, Greece. *Int. J. Biometeorol.* **1982**, *26*, 53–59. [CrossRef]
56. Tsitoura, M.; Tsoutsos, T.; Daras, T. Evaluation of Comfort Conditions in Urban Open Spaces. Application in the Island of Crete. *Energy Convers. Manag.* **2014**, *86*, 250–258. [CrossRef]
57. Matzarakis, A.; Mayer, H. Heat Stress in Greece. *Int. J. Biometeorol.* **1997**, *41*, 34–39. [CrossRef]
58. Kambezidis, H.D.; Psiloglou, B.E.; Varotsos, K.V.; Giannakopoulos, C. Climate Change and Thermal Comfort in Greece. *Climate* **2021**, *9*, 10. [CrossRef]
59. Kambezidis, H.D.; Psiloglou, B.E.; Kaskaoutis, D.G.; Karagiannis, D.; Petrinoli, K.; Gavriil, A.; Kavadias, K. Generation of typical meteorological years for 33 locations in Greece: Adaptation to the needs of various applications. *Theor. Appl. Clim.* **2020**, *141*, 1313–1330. [CrossRef]
60. Giles, B.D.; Balafoutis, C.; Maheras, P. Too Hot for Comfort: The Heatwaves in Greece in 1987 and 1988. *Int. J. Biometeorol.* **1990**, *34*, 98–104. [CrossRef]
61. Paliatsos, A.G.; Nastos, P.T. Relation between air pollution episodes and discomfort index in the greater Athens area, Greece. *Glob. Nest J.* **1999**, *1*, 91–97. [CrossRef]
62. Tselepidaki, I.; Santamouris, M.; Moustris, C.; Poulopoulou, G. Analysis of the Summer Discomfort Index in Athens, Greece, for Cooling Purposes. *Energy Build.* **1992**, *18*, 51–56. [CrossRef]
63. Bartzokas, A.; Lolis, C.J.; Kassomenos, P.A.; McGregor, G.R. Climatic Characteristics of Summer Human Thermal Discomfort in Athens and Its Connection to Atmospheric Circulation. *Nat. Hazards Earth Syst. Sci.* **2013**, *13*, 3271–3279. [CrossRef]
64. Matzarakis, A.; Nastos, P.T. Human-biometeorological assessment of heat waves in Athens. *Theor. Appl. Climatol.* **2011**, *105*, 99–106. [CrossRef]
65. Nastos, P.T.; Matzarakis, A. The Effect of Air Temperature and Human Thermal Indices on Mortality in Athens, Greece. *Theor. Appl. Climatol.* **2012**, *108*, 591–599. [CrossRef]
66. Pantavou, K.; Santamouris, M.; Asimakopoulos, D.; Theoharatos, G. Empirical Calibration of Thermal Indices in an Urban Outdoor Mediterranean Environment. *Build. Environ.* **2014**, *80*, 283–292. [CrossRef]
67. Pantavou, K.; Theoharatos, G.; Santamouris, M.; Asimakopoulos, D. Outdoor Thermal Sensation of Pedestrians in a Mediterranean Climate and a Comparison with UTCI. *Build. Environ.* **2013**, *66*, 82–95. [CrossRef]
68. Katavoutas, G.; Founda, D. Intensification of Thermal Risk in Mediterranean Climates: Evidence from the Comparison of Rational and Simple Indices. *Int. J. Biometeorol.* **2019**, *63*, 1251–1264. [CrossRef] [PubMed]
69. International Meteorological Organisation (IMO). *Provisional Guide to International Meteorological Instruments and Observing Practice*; IMO No. 78 Technical Report, Chapters 1 to 10; International Meteorological Organisation: Lausanne, Switzerland, 1950.
70. World Meteorological Organization (WMO). *Guide to Meteorological Instruments and Methods of Observation*, 7th ed.; WMO-No. 8 Technical Report; World Meteorological Organization (WMO): Geneva, Switzerland, 2008.
71. World Meteorological Organization (WMO). *Guide to Meteorological Instruments and Methods of Observation: Volume I—Measurements of Meteorological Variables*; WMO-No. 8; World Meteorological Organization (WMO): Geneva, Switzerland, 2024.
72. Eginitis, D. *The Climate of Greece, Part A*; P. Sakkelariou Editions: Athens, Greece, 1907; pp. 227–228. (In Greek)

73. Founda, D.; Kambezidis, H.D.; Petrakis, M.; Zanis, P.; Zerefos, C. A correction of the recent air-temperature record at the historical meteorological station of the National Observatory of Athens (NOA) due to instrument change. *Theor. Appl. Climatol.* **2009**, *97*, 385–389. [CrossRef]
74. McGregor, G.R.; Vanos, J.K. Heat: A primer for public health researchers. *Public Health* **2018**, *161*, 138–146. [CrossRef]
75. Psiloglou, B.E.; Larissi, I.K.; Petrakis, M.; Paliatsos, A.G.; Antoniou, A.; Viras, L.G. Case Studies on Summertime Measurements of O_3, NO_2, and SO_2 with a DOAS System in an Urban Semi-Industrial Region in Athens, Greece. *Environ. Monit. Assess.* **2013**, *185*, 6565–6576. [CrossRef]
76. Kallos, G.; Kassomenos, P.; Pielke, R. Synoptic and mesoscale weather conditions during air pollution episodes in Athens, Greece. *Bound. Layer Meteorol.* **1993**, *62*, 163–184. [CrossRef]
77. Kassomenos, P.; Kotroni, V.; Kallos, G. Analysis of the climatological and air quality observations from Greater Athens Area. *Atmos. Environ.* **1995**, *29*, 3671–3688. [CrossRef]
78. Tung, A. The City of the Gods Besieged. In *Preserving the World's Great Cities: The Destruction and Renewal of the Historic Metropolis*; Three Rivers Press: New York, NY, USA, 2001; pp. 260, 263, 265. ISBN 0-609-80815-X.
79. Hellenic Statistical Authority (ELSTAT). *2021 Population Census (Greek Language PDF)*; Hellenic Statistical Authority: Athens, Greece, 2021. Available online: https://www.statistics.gr/en/2021-census-pop-hous (accessed on 10 July 2025).
80. Hellenic Statistical Authority (ELSTAT). *Census 2022 Greece: Population and Housing Census (Greek Language PDF)*; Hellenic Statistical Authority: Athens, Greece, 2022. Available online: https://elstat-outsourcers.statistics.gr/Census2022_GR.pdf (accessed on 10 July 2025).
81. National Centre for Social Research. Panorama of Greek Census Data. Available online: https://panorama.statistics.gr/en/ (accessed on 10 July 2025).
82. Athens Social Atlas. Available online: https://www.athenssocialatlas.gr (accessed on 10 July 2025).
83. Metaxas, D.A.; Bartzokas, A.; Vitsas, A. Temperature Fluctuations in the Mediterranean Area during the Last 120 Years. *Int. J. Climatol.* **1991**, *11*, 897–908. [CrossRef]
84. Founda, D. Evolution of the Air Temperature in Athens and Evidence of Climatic Change: A Review. *Adv. Build. Energy Res.* **2011**, *5*, 7–41. [CrossRef]
85. American Society of Heating, Refrigeration and Air-Conditioning Engineers (ASHRAE). *Heating, Ventilating, Air-Conditioning, Guide No. 33*; ASHRAE: New York, NY, USA, 1955.
86. Thom, E.C. A New Concept for Cooling Degree-Days. *Air Cond. Heat. Vent.* **1957**, *54*, 73–80.
87. Giannakopoulos, C.; Kostopoulou, E.; Varotsos, K.V.; Tziotziou, K.; Plitharas, A. An Integrated Assessment of Climate Change Impacts for Greece in the Near Future. *Reg. Environ. Change* **2011**, *11*, 829–843. [CrossRef]
88. Rana, R.; Kusy, B.; Jurdak, R.; Wall, J.; Hu, W. Feasibility Analysis of Using Humidex as an Indoor Thermal Comfort Predictor. *Energy Build.* **2013**, *64*, 17–25. [CrossRef]
89. Steadman, R.G. A Universal Scale of Apparent Temperature. *J. Clim. Appl. Meteorol.* **1984**, *23*, 1674–1687. [CrossRef]
90. NOAA (National Oceanic and Atmospheric Administration). National Weather Service Glossary. 2009. Available online: http://www.weather.gov/glossary/ (accessed on 12 October 2012).
91. Steadman, R.G. Norms of Apparent Temperature in Australia. *Aust. Meteorol. Mag.* **1994**, *43*, 1–16.
92. NWS (National Weather Service). Meteorological Conversions and Calculations: Heat Index Calculator. 2011. Available online: https://www.wpc.ncep.noaa.gov/html/heatindex.shtml (accessed on 12 October 2011).
93. NOAA (National Oceanic and Atmospheric Administration). Heat: A Major Killer. 2012. Available online: http://www.nws.noaa.gov/om/heat/index.shtml (accessed on 12 October 2012).
94. United States National Weather Service, Pueblo, Colorado. Heat Index. Available online: https://web.archive.org/web/20110629041320/http://www.crh.noaa.gov/pub/heat.php (accessed on 10 July 2025).
95. The Intergovernmental Panel on Climate Change (IPCC). *Managing the Risks of Extreme Events and Disasters to Advance Climate Change Adaptation (SREX)*; Field, C.B., Barros, V., Stocker, T.F., Qin, D., Dokken, D.J., Ebi, K.L., Mastrandrea, M.D., Mach, K.J., Plattner, G.K., Allen, S.K., et al., Eds.; Cambridge University Press: New York, NY, USA, 2012. Available online: https://www.ipcc.ch/report/managing-the-risks-of-extreme-events-and-disasters-to-advance-climate-change-adaptation/ (accessed on 28 August 2025).
96. World Meteorological Organization & World Health Organization (WMO/WHO). *Heatwaves and Health: Guidance on Warning-System Development*; WMO No. 114 Technical Report, Chapter 7; McGregor, G.R., Bessemoulin, P., Ebi, K., Menne, B., Eds.; World Meteorological Organization: Geneva, Switzerland, 2015. Available online: https://www.who.int/publications/m/item/heatwaves-and-health{-}{-}guidance-on-warning-system-development (accessed on 28 August 2025).
97. D'Ippoliti, D.; Michelozzi, P.; Marino, C.; de'Donato, F.; Menne, B.; Katsouyanni, K.; Kirchmayer, U.; Analitis, A.; Medina-Ramón, M.; Paldy, A.; et al. The impact of heat waves on mortality in 9 European cities: Results from the EuroHEAT project. *Environ. Health* **2010**, *9*, 37. [CrossRef] [PubMed]
98. Habeeb, D.; Vargo, J.; Stone, B. Rising heat wave trends in large US cities. *Nat. Hazards* **2015**, *76*, 1651–1665. [CrossRef]

99. Spector, J.T.; Masuda, Y.J.; Wolff, N.H.; Calkins, M.; Seixas, N. Heat exposure and occupational injuries: Review of the literature and implications. *Curr. Environ. Health Rep.* **2019**, *6*, 286–296. [CrossRef] [PubMed]
100. Vicedo-Cabrera, A.M.; Scovronick, N.; Sera, F.; Royé, D.; Schneider, R.; Tobias, A.; Astrom, C.; Guo, Y.; Honda, Y.; Hondula, D.M.; et al. The burden of heat-related mortality attributable to recent human-induced climate change. *Nat. Med.* **2020**, *27*, 1027–1034. [CrossRef]
101. Perkins-Kirkpatrick, S.E.; Lewis, S.C. Increasing trends in regional heatwaves. *Nat. Commun.* **2020**, *11*, 3357. [CrossRef]
102. Schwingshackl, C.; Sillmann, J.; Vicedo-Cabrera, A.M.; Sandstad, M.; Aunan, K. Heat stress indicators in CMIP6: Estimating future trends and exceedances of impact-relevant thresholds. *Earth's Future* **2021**, *9*, e2020EF001885. [CrossRef]
103. Russo, S.; Dosio, A.; Graversen, R.G.; Sillmann, J.; Carrao, H.; Dunbar, M.B.; Vogt, J.V. Magnitude of extreme heat waves in present climate and their projection in a warming world. *J. Geophys. Res. Atmos.* **2014**, *119*, 12500–12512. [CrossRef]
104. Katavoutas, G.; Founda, D.; Varotsos, K.V.; Giannakopoulos, C. Diurnal Temperature Range and Its Response to Heat Waves in 16 European Cities—Current and Future Trends. *Sustainability* **2023**, *15*, 12715. [CrossRef]

Disclaimer/Publisher's Note: The statements, opinions and data contained in all publications are solely those of the individual author(s) and contributor(s) and not of MDPI and/or the editor(s). MDPI and/or the editor(s) disclaim responsibility for any injury to people or property resulting from any ideas, methods, instructions or products referred to in the content.